

UNIVERSITY OF NORTH DAKOTA

Grand Forks



Developing Balanced Mix Design Gyration (N_{design}) for North Dakota's HMA Pavements

Final Report

2022

By:

Dr. Nabil Suleiman, Principal Investigator
Dr. Daba Gedafa, Co-Principal Investigator

Disclaimer

The contents of this report reflect the views of the author or authors who are responsible for the facts and accuracy of the data presented herein. The contents do not reflect the official views of the North Dakota Department of Transportation or the Federal Highway Administration. This report does not constitute a standard, specification, or regulation.

ACKNOWLEDGMENT

The Principal investigators (PI and Co-PI) appreciate the funding provided by the NDDOT that made this research study possible. The PI's also wish to thank the Materials and Research Division staff for their insights and for collecting and delivering the study materials. The PI's recognize the contributions of Mr. Anjo Mate, who conducted many of the laboratory tests at part of his Master's degree requirements. Special thanks are due to Mr. Bruce Dockter, laboratory manager at the Civil Engineering Department at the University of North Dakota, who assisted in laboratory testing, especially the DCT and SCB testing protocols.

TABLE OF CONTENTS

| | |
|---|-------------|
| ACKNOWLEDGEMENTS | iii |
| TABLE OF CONTENTS | iv |
| LIST OF FIGURES | vi |
| LIST OF TABLES | vii |
| LIST OF EQUATIONS..... | vii |
| EXECUTIVE SUMMARY | viii |
| 1. INTRODUCTION..... | 1 |
| 1.1 Background | 1 |
| 1.2 Major Asphalt Distresses in North Dakota..... | 1 |
| 1.2.1 Rutting..... | 1 |
| 1.2.2 Fatigue Cracking..... | 1 |
| 1.2.3 Low Temperature (Thermal) Cracking..... | 2 |
| 1.3 Problem Statement and Motivation..... | 3 |
| 1.4 Objectives..... | 3 |
| 2. LITERATURE REVIEW | 4 |
| 2.1 Balanced Mix Design and Calibration Efforts | 4 |
| 2.2 Asphalt Performance Tests..... | 5 |
| 2.2.1 Asphalt Pavement Analyzer Test (APA)..... | 5 |
| 2.2.2 Disk-Shaped Compaction Test (DCT)..... | 6 |
| 2.2.3 Semi-Circular Bending Test (SCB)..... | 7 |
| 2.3 Durability of Hot Mix Asphalt (HMA) | 8 |
| 2.4 Effects of Asphalt Binder on Pavement Performance..... | 8 |
| 2.4.1 Effect of N_{design} on Pavement Performance | 8 |
| 2.4.2 Rutting..... | 9 |
| 2.4.3 Fatigue Cracking..... | 11 |
| 2.4.4 Low Temperature Cracking..... | 12 |
| 3. METHODOLOGY | 14 |
| 3.1 General | 14 |
| 3.2 Project Selection..... | 14 |
| 3.3 Mix Preparations and Computations | 14 |
| 3.3.1 Mass Determination of Aggregate and Asphalt Binder..... | 14 |
| 3.3.2 Theoretical Maximum Specific Gravity (G_{mm})..... | 15 |

| | |
|---|-----------|
| 3.3.3 Mixing and Compaction of Asphalt Specimens. | 17 |
| 3.3.4 Bulk Specific Gravity of the Mix (G_{mb})..... | 19 |
| 3.3.5 Percent (%) Air Voids of the Specimen (V_a). | 20 |
| 3.4 Performance Testing..... | 20 |
| 3.4.1 APA Test..... | 21 |
| 3.4.2 DCT Test..... | 21 |
| 3.4.3 SCB Test. | 23 |
| 4. RESULTS AND DISCUSSIONS | 25 |
| 4.1 Theoretical Maximum Specific Gravity..... | 25 |
| 4.2 Determination of Optimum Asphalt Content | 28 |
| 4.3 Rutting Performance..... | 35 |
| 4.4 Low Temperature Cracking Performance | 37 |
| 4.5 Fatigue Cracking Performance | 39 |
| 4.6 Statistical Analysis | 41 |
| 5. CONCLUSIONS AND RECOMMENDATIONS..... | 44 |
| 6. REFERENCES..... | 46 |

LIST OF FIGURES

| | |
|---|----|
| Figure 1. Rutting in a Two-Lane Asphalt Pavement | 1 |
| Figure 2. Images of Fatigue Cracking in Asphalt Pavement | 2 |
| Figure 3. Images of Thermal Cracking in Asphalt Pavement..... | 2 |
| Figure 4. Asphalt Pavement Analyzer | 5 |
| Figure 5. Disc-Shaped Compaction Test (DCT) Sample Dimension..... | 6 |
| Figure 6. Semi Circular Bending (SCB) Sample Test Dimension..... | 7 |
| Figure 7. Relative Performance Versus Asphalt Content | 8 |
| Figure 8. Number of Gyration Versus Asphalt Content..... | 9 |
| Figure 9. Asphalt Pavement displaced under the tires | 10 |
| Figure 10. Samples Ready for Theoretical Maximum Specific Gravity (G_{mm}) testing | 16 |
| Figure 11. Set-up of Bowl and Vacuum Gauge..... | 16 |
| Figure 12. Theoretical Maximum Specific Gravity (G_{mm}) Experiment Set-up | 17 |
| Figure 13. Mixing Bowls and Wire Whisks | 18 |
| Figure 14. SuperPave Gyrotory Compactor..... | 18 |
| Figure 15. Sample Asphalt Plug Weighed in Air and Sample Submerged Under Water. | 19 |
| Figure 16. Asphalt Samples ready for G_{sb} Experiment..... | 20 |
| Figure 17. Cutting, Drilling and Sawing Machines | 21 |
| Figure 18. DCT Samples Ready for Testing..... | 22 |
| Figure 19. DCT Sample Set-Up..... | 22 |
| Figure 20. Typical Load vs $CMOD_{fit}$ | 23 |
| Figure 21. SCB Samples Ready For Testing | 23 |
| Figure 22. SCB Sample Set-Up | 24 |
| Figure 23. Typical Load Vs Displacement | 24 |
| Figure 24. Air Voids vs Binder Content (75 Gyration) – Rugby Mix | 29 |
| Figure 25. Air Voids vs Binder Content (65 Gyration) – Rugby Mix | 30 |
| Figure 26. Air Voids vs Binder Content (55 Gyration) – Rugby Mix | 30 |
| Figure 27. Air Voids vs Binder Content (75 Gyration) – Eddy Mix..... | 32 |
| Figure 28. Air Voids vs Binder Content (65 Gyration) – Eddy Mix..... | 32 |
| Figure 29. Air Voids vs Binder Content (55 Gyration) – Eddy Mix..... | 33 |
| Figure 30. Air Voids vs Binder Content (75 Gyration) – Fargo Mix..... | 33 |
| Figure 31. Air Voids vs Binder Content (65 Gyration) – Fargo Mix..... | 33 |
| Figure 32. Air Voids vs Binder Content (50 Gyration) – Fargo Mix..... | 34 |
| Figure 33. Air Voids vs Binder Content (75 Gyration) – GF Mix | 34 |
| Figure 34. Air Voids vs Binder Content (65 Gyration) – GF Mix | 34 |
| Figure 35. Air Voids vs Binder Content (50 Gyration) – GF Mix | 35 |
| Figure 36. Average Rut Resistance Performance Summary..... | 36 |
| Figure 37. Overall Low Temperature Cracking Performance Results | 38 |
| Figure 38. Typical Sample After DCT Test..... | 39 |
| Figure 39. Fatigue Cracking Performance Summary | 40 |
| Figure 40. Flexibility Index (FI) Performance Summary | 40 |
| Figure 41. Typical Sample After SCB Test..... | 41 |

LIST OF TABLES

| | |
|--|----|
| Table 1. NDDOT Mix Properties..... | 4 |
| Table 2 Project Summary..... | 14 |
| Table 3. Rugby Mix Batch Weights | 14 |
| Table 4. Eddy Mix Batch Weights..... | 15 |
| Table 5. Fargo Mix Batch Weights..... | 15 |
| Table 6. Grand Forks Mix Batch Weights | 15 |
| Table 7. G_{mm} Results for Rugby’s Mix..... | 25 |
| Table 8. G_{mm} Results for Eddy’s Mix | 25 |
| Table 9. G_{mm} Results for Fargo’s Mix | 26 |
| Table 10. G_{mm} Results for Grand Forks Mix | 27 |
| Table 11. UND Lab G_{mm} Results VS NDDOT Mix Design Values | 28 |
| Table 12. Air Voids Calculations VS Asphalt Contents at 75 Gyration (Rugby)..... | 29 |
| Table 13. Air Voids Calculations VS Asphalt Contents at 65 Gyration (Rugby)..... | 29 |
| Table 14. Air Voids Calculations VS Asphalt Contents at 55 Gyration (Rugby)..... | 29 |
| Table 15. Air Voids Calculations VS Asphalt Contents at 75 Gyration (Eddy)..... | 30 |
| Table 16. Air Voids Calculations VS Asphalt Contents at 65 Gyration (Eddy)..... | 31 |
| Table 17. Air Voids Calculations VS Asphalt Contents at 55 Gyration (Eddy)..... | 31 |
| Table 18. Air Voids Calculations VS Asphalt Contents at 75 Gyration (Fargo)..... | 31 |
| Table 19. Air Voids Calculations VS Asphalt Contents at 65 Gyration (Fargo)..... | 31 |
| Table 20. Air Voids Calculations VS Asphalt Contents at 50 Gyration (Fargo)..... | 31 |
| Table 21. Air Voids Calculations VS Asphalt Contents at 75 Gyration (GF)..... | 31 |
| Table 22. Air Voids Calculations VS Asphalt Contents at 65 Gyration (GF)..... | 32 |
| Table 23. Air Voids Calculations VS Asphalt Contents at 50 Gyration (GF)..... | 32 |
| Table 24. Optimal Binder Content and G_{mm} Values for All Mixes and Gyration Levels | 35 |
| Table 25. Rut Resistance Performance Summary for the Rugby Mix..... | 36 |
| Table 26. Rut Resistance Performance Summary for the Eddy Mix..... | 36 |
| Table 27. Rut Resistance Performance Summary for the Fargo Mix..... | 36 |
| Table 28. Rut Resistance Performance Summary for the GF Mix | 36 |
| Table 29. Low Temperature Performance DCT Test Summary Results - Rugby | 37 |
| Table 30. Low Temperature Performance DCT Test Summary Results - Eddy | 37 |
| Table 31. Low Temperature Performance DCT Test Summary Results - Fargo | 37 |
| Table 32. Low Temperature Performance DCT Test Summary Results - GF..... | 37 |
| Table 33. Fatigue Cracking and FI Performance Summary - Rugby | 39 |
| Table 34. Fatigue Cracking and FI Performance Summary - Eddy..... | 39 |
| Table 35. Fatigue Cracking and FI Performance Summary - Fargo..... | 39 |
| Table 36. Fatigue Cracking and FI Performance Summary - GF..... | 40 |
| Table 37. Single Factor ANOVA Analysis on the APA Rutting Results..... | 42 |
| Table 38. Single Factor ANOVA Analysis on the DCT Fracture Energy Results | 42 |
| Table 39. Single Factor ANOVA Analysis on the SCB FI Results..... | 43 |
| Table 40. Rutting, LTC, and FC Performance for all Mixes and Gyration Levels | 45 |

LIST OF EQUATIONS

| | |
|---|----|
| Equation 1. Total Amount of Aggregates and Asphalt Binder..... | 15 |
| Equation 2. Theoretical Maximum Specific Gravity of the Mix | 17 |

| | |
|--|----|
| Equation 3. Bulk Specific Gravity of the Mix | 19 |
| Equation 4. Percent Air Voids | 20 |
| Equation 5. Flexibility Index | 23 |

EXECUTIVE SUMMARY

Various number of gyrations (N_{design}) for SuperPave mix design in North Dakota were investigated for the North Dakota Department of Transportation (NDDOT) to produce mixes representing field conditions of specified traffic volumes and pavement classes. Since SuperPave mix design was mainly developed for high volume roads, various research suggests that there is a need to develop a new mix design criterion for medium and low volume traffic. For low volume roads, durability performance of the HMA is generally affected by the environment and not by heavy traffic or large traffic volumes. High N_{design} numbers tend to lower the asphalt binder, thus lower the durability of the asphalt mix. In contrast, if N_{design} is reduced, it tends to increase the asphalt binder, thus increases durability of the asphalt mix.

The main objective of this study was to determine the effect of varying number of design gyrations on the hot mix asphalt (HMA) performance in terms of rutting, low-temperature cracking, and fatigue cracking resistances. Project mix samples were constructed and tested based on N_{design} values of 75, 65, and 55 (or 50) gyrations. The sample matrix included fine aggregate angularity (FAA) values of 45, 43, and 40. It also included asphalt binders of PG 58S-28, PG 58H-34, and PG 58H-28.

The Analysis of Variance (ANOVA) was performed on the results and showed that the results within and across gyration levels were significantly different, thus can be compared. Test results showed that lower number of gyrations and higher binder content resulted in higher fatigue cracking and thermal cracking resistances. Even-though, lowering the number of gyrations decreased the rutting resistance, the overall rut resistance performance stayed within acceptable levels.

Therefore, the recommended N_{design} for the high-end pavements (i.e, FAA 45 and PG 58H-28 or PG 58H-34) is 65 gyrations while for intermediate and low-end pavements (i.e., FAA 43 or 40 and PG 58S-28), the recommended number of gyrations is 50.

1. INTRODUCTION

1.1 Background

North Dakota is one of the coldest states based on average temperature, which is 40.4 degrees Fahrenheit. The coldest temperature in the area ever recorded was - 60 degrees Fahrenheit in 1936. On the other hand, summer temperatures exceed 100 degrees Fahrenheit. Due to these intense conditions, asphalt pavements in the area tend to be prone to rutting, fatigue cracking, and thermal cracking.

1.2 Major Asphalt Distresses in North Dakota

1.2.1 Rutting.

Rutting is defined as the permanent deformation or consolidation that accumulates in the asphalt (Liley, 2018). Ruts can be usually seen during summer where the temperature is high, and when the binder on the surface of older asphalt roads begin to stick to the bottom of the shoes. It occurs because the aggregate and binder in asphalt roads can move. Ruts are visible after rain when they are filled with water (Washington Asphalt Pavement Association, 2010). Ruts are formed when a truck drives over a road that lacks internal strength to resist permanent deformation under stress imposed by the loaded wheel of vehicle tires (Liley, 2018). If this distress is not treated, it can cause accidents to drivers and passengers. Figure 1 shows a severe rutting distress in asphalt pavement.



Figure 1. Rutting in a Two-lane Asphalt Pavement (Pavement Interactive, 2009)

1.2.2 Fatigue Cracking.

Fatigue or alligator cracking is a series of interconnected cracks caused by fatigue failure of hot mix asphalt under repetition of vehicle loadings (West et al, 2018). For thinner pavements, cracking starts at the bottom of the HMA layer where tensile stress is the highest and then proliferate towards the surface as one or more longitudinal cracks which is called bottom up or classic fatigue cracking. In contrast, thicker pavements essentially start from the top in areas of high localized tensile stress resulting from tire to pavement interaction and asphalt binder aging. After the said repeated loadings, longitudinal cracks connect forming many sided sharp angled pieces that turns into a pattern resembling the back of an alligator or crocodile (Washington

Asphalt Pavement Association, 2010). Furthermore, West et al. (2018) added that fatigue cracking is also affected by aging that correlates with embrittlement of asphalt binder. Due to continuous loading and climate factors to asphalt pavement, it reduces its structural integrity causing it to crack and may become a pothole that would risk its users. Figure 2, as shown, will start as a crack and then propagate looking like a back of an alligator.



Figure 2. Images of Fatigue Cracking in Asphalt Pavement (Pavement Interactive, 2009)

1.2.3 Low Temperature (Thermal) Cracking.

Thermal or transverse cracking is the distress that is found in asphalt pavements in low temperature climates. Transverse cracking is a common problem and a safety hazard because the roads are constantly in use. Cracks develop when temperatures drop, and the asphalt pavement shrinks and contracts. This is the reason why it is also referred to as thermal cracking (Bradshaw, 2016). As the asphalt begins to tighten, tensile stress builds up to a critical point at which cracks are formed (Minnesota Department of Transportation, 2014). Aschenbrener (1995) added that transverse cracks are relatively perpendicular to the centerline of the pavement. Cracks start usually on the surface of the pavement and then gradually sink deeper below the surface like figure 3 shown below.



Figure 3. Images of Thermal Cracking in Asphalt Pavement (Pavement Interactive, 2009)

1.3 Problem Statement and Motivation

In the past few decades, North Dakota has been focusing on rutting failure in asphalt pavement. That lead to maintaining the compaction effort (N_{design}) of SuperPave mixes at 75 gyrations for all pavement classes regardless of traffic level. According to North Dakota Department of Transportation (NDDOT) engineers and materials coordinators, rutting was always in check throughout the state.

NDDOT experts started to recognize that the rut resistant pavements constructed were failing because they were dry, brittle, and in some cases have various permeability problems because of density issues. Durability in asphalt pavement needs to be addressed as suggested by some engineers from around the state. The initial solution is by lowering the number of gyrations allowing binder contents to increase while aggregate gradation (structure) is maintained. There were attempts by some districts to reduce N_{design} on projects from 75 to 65 or even 50 gyrations on low volume roads where rutting was not a concern. District engineers noticed that binder content was increased by 0.1 to 0.2 percent, which was expected to help with durability issues in asphalt pavements.

Low temperature cracking and fatigue cracking and other durability related modes of failure are the root causes of damage in asphalt pavements here in North Dakota's lower pavement classifications. Lowering the number of gyrations, while keeping aggregate gradations the same will probably be the solution to this dilemma. Conclusively, this will lead to an increase in binder content, voids in mineral aggregate, and film thickness, but surely, this is expected to help with durability issues in North Dakota.

1.4 Objectives

The main objectives of this research study are the following:

- a) Investigate the effect of reduced number of design gyrations (75, 65, 55, or 50) on the HMA performance of various pavement classes (high, intermediate, and low) in terms of rutting, low-temperature cracking (LTC), and fatigue cracking (FC) resistances.
- b) Develop an appropriate number of gyrations (N_{design}) that will produce balanced mix designs that will be recommended for various pavement classes based on their tested performances.

2. LITERATURE REVIEW

2.1 Balanced Mix Design and Calibration Efforts

In early 1990s, the Superior Performing Asphalt Pavement System (SuperPave) mix design method was developed from the Strategic Highway Research Program (SHRP). The primary focus of SuperPave is to limit detrimental distresses of asphalt pavements. It takes account of the changes in environmental conditions, traffic loading, and axle configurations. Additionally, SuperPave assesses asphalt binder, aggregate properties, mixture analysis, and volumetric properties in HMA (Williams, et. al., 2016). Volumetric analysis of HMAs is mainly used to determine optimum asphalt content in the mixture. SuperPave gyratory compactor (SGC) is generally the compaction device used to compact laboratory specimens. As it is heavily dependent on traffic levels, it is generally expressed as 18,000 lbs (Williams, et. al., 2016). HMA samples are generally compacted in an internal angle of gyration of 1.16° (external angle 1.25°) with a constant pressure of 600 kilopascal (kPa) (Prowell & Brown, 2007). NDDOT adopted compaction effort for different levels and was denoted as N_{initial} , N_{design} , and N_{max} as shown in Table 1 (NDDOT, Standard Specifications for Road and Bridge Design, 2020).

Table 1. NDDOT Mix Properties

| Property | FAA 40 | FAA 41 | FAA 42 | FAA 43 | FAA 44 | FAA 45 |
|---|---|--------|--------|--------|--------|--------|
| Fractured Particles in Course Aggregate (minimum) | 75% | 75% | 75% | 75% | 85% | 85% |
| Fine Aggregate Angularity (minimum) | 40% | 41% | 42% | 43% | 44% | 45% |
| Gyratory Effort, # of Gyration | $N_{\text{ini}} = 7, N_{\text{des}} = 75, N_{\text{max}} = 115$ | | | | | |
| Voids filled with Bitumen | 65-78% | 65-78% | 65-78% | 65-78% | 65-75% | 65-75% |
| % G_{mm} @ N_{ini} (maximum) | 90.5% | 90.5% | 89% | 89% | 89% | 89% |

In 2015, Federal Highway Agency (FHWA) Expert Task Group on Mixtures and Construction formed a Balanced Mix Design (BMD) Task Force. The objective of the BMD group was to assess “asphalt mix design using performance tests on appropriately conditioned specimens that address multiple modes of distress taking into consideration mix aging, traffic, climate and location within the pavement structure.” (National Center for Asphalt Technology, 2017).

As the N_{design} is used to simulate field compaction during construction, there have been reports that it produced air voids that are unable to reach ultimate pavement density within the initial 2 to 3 years of post-construction, potentially impacting long term performance of HMAs. Regarding durability problems of asphalt pavement, there had been various research to investigate the current levels with existing mixes and did recommendations to calibrate or identify the optimum N_{design} with the use of performance tests.

Aguilar-Moya et al. (2001) established that the number of design gyrations using the SuperPave Gyratory Compactor could be reduced significantly to optimize fatigue life of the asphalt mixes. The study used the relative performance base approach as applied to two performance-related tests such as the Hamburg Wheel Tracking Device (HWTB) and the four-point bending beam. It was observed that in 100 gyrations which is the current specification for 1

million to 30 million ESALs, the rutting performance in the laboratory was very high (75% to 95% relative performance); however, fatigue performance is typically low (varying from 20% to 70% relative performance). Aguilar-Moya et al. (2001) saw from the average relative performance of all the mixes tested, that generally 55 to 85 gyrations on the SGC do optimize the performance of the asphalt mixes. However, these recommendations were based on limited sample mixes.

Low volume roads (LVRs) are defined as roads lying outside of built-up areas of cities, towns, and communities and shall have an Equivalent Single Axle Loading of less than 300,000. To increase durability and longevity of LVR asphalt pavements, various research efforts were made to calibrate N_{design} for low volume roads.

Cross & Choho Lee (2000) evaluated void properties at the original and revised N_{design} gyrations and the effect of reducing the ram pressure from 600 kPa to 400 kPa. SuperPave Gyrotory Compactor (SGC) was used to compact the field mix to establish the number of gyrations required to reach field density. They wanted to prove that N_{design} values were inaccurate for all levels of traffic. It was found that N_{design} was developed with higher quality aggregates that were typically found in Kansas and the Midwest (Cross & Choho Lee, 2000). The primary problem in meeting the SuperPave Level 1 mix requirements has typically been Voids in Mineral Aggregates (VMA), which is explained as a volumetric property and a function of compactive effort. They utilized the Asphalt Pavement Analyzer (APA) with traffic less than one million ESALs. It was observed that the use of SGC resulted in an average reduction in VMA of 1.2% to 1.9% when compared to 50-blow Marshall compaction. Thus, SGC resulted in an average reduction in optimum asphalt content of 0.5% to 0.8% when compared to Marshall compaction (Cross & Choho Lee, 2000). Cross & Choho Lee (2000) recommended that the effect of reducing the VMA requirement on durability of bituminous mixes should be evaluated. Also, it may be possible to reduce the VMA requirement by 0.5% to 1% without sacrificing the performance of low volume pavements.

2.2 Asphalt Performance Tests

2.2.1 Asphalt Pavement Analyzer Test (APA).

Asphalt pavement analyzer (APA) is a wheel tracking device that is used to run simulative test that measures HMA qualities by rolling a small loaded wheel device repeatedly across a mixed asphalt specimen. The APA is a second-generation device that was originally developed in the 1980's as the Georgia Loaded Wheel tester (GLWT). Figure 4 is a modification of GLWT and was first made in 1996 by Pavement Technology, Inc. Since then, APA has been utilized to evaluate rutting, fatigue, and moisture resistance of HMA mixtures.



Figure 4. Asphalt Pavement Analyzer

Kandhal & Mallick (1999), studied the APA as a tool for evaluation of rut potential of HMA with different aggregates, gradations, nominal maximum size aggregates, asphalt binders, mixes prepared with granite, limestone, and gravel. Tests were conducted under dry conditions with mixes obtained from high, intermediate and low rutting pavements. They concluded that gradation is the single most important property that determines the stability of a mix. Additionally, they observed that the type of aggregate top size has significant effect on rutting potential. They also found that APA is sensitive to aggregate gradation and asphalt binder PG grade. Lastly, it was concluded that APA has a potential to accurately predict the rutting potential of hot mix asphalt mixes.

As Minnesota Department of Transportation (MNDOT) was looking to purchase APA, Skok, et. al. (2000) made an evaluation of APA. To determine if APA was a good tool for evaluating the rutting of asphalt, they developed a questionnaire and sent out to members of APA users' group. Majority of the responses indicated that most of the users were satisfied with the results and reliability of the APA. So, it was concluded that MNDOT must have the APA.

2.2.2 Disk-Shaped Compaction Test (DCT).

Disk-shaped compaction test (DCT) is a fracture test that predicts fracture resistance of asphalt concrete from conventional engineering parameters, such as modulus and tensile strength. To fully understand the crack initiation and propagation in asphalt concrete, fracture mechanics must be understood to understand the evolution of performance-based pavement design. Fracture mechanics had been used since the early 1970's which was utilized to analyze the fracture behavior of concrete (Wagoner, et. al., 2005). Since then, DCT was used to evaluate the low temperature cracking of asphalt which is the most prevalent pavement distress especially in the cold climate areas (Wagoner, et. al., 2005).

Wagoner, et. al. (2005) described the development of a practical test to obtain the fracture energy of asphalt and field specimens. They found out that with the use of DCT geometry, it was considered a practical geometry that can be fabricated from cylindrical cores from in-place pavements or gyratory compacted specimens. The DCT geometry was developed using the ASTM E399 specification. They found out that DCT geometry, as shown in Figure 5, to be promising for obtaining the fracture energy of asphalt concrete that is amenable for both laboratory and field core specimens.

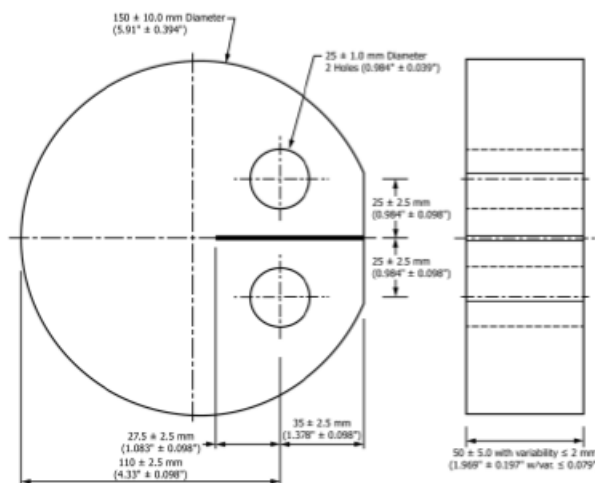


Figure 5. Disc-Shaped Compaction Test (DCT) Sample Dimension (Wagoner, et. al. 2005)

2.2.3 Semi-Circular Bending Test (SCB).

Semi-Circular Bending (SCB) test is another fracture test based on linear-elastic fracture mechanics (LEFM). It was adopted by pavement engineers to understand fracture characteristics of different asphalt mixtures which led to the development of standard protocols for monotonic loading conditions. The SCB test has shown great potential research for determining the mixed mode fracture behavior of asphalt mixtures by simply adjusting the inclination angle of the notch or the space between two supports. Test specimens for SCB are either made by an SGC or taken from cores drilled from the field. The disc is sawn into two equal parts resulting in two semi-circular samples as shown in the Figure 6.

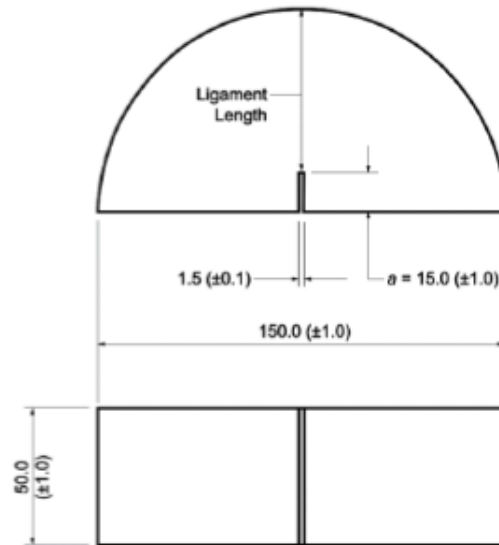


Figure 6. Semi Circular Bending (SCB) Sample Test Dimension (Nsengiyumva, et. al. 2015)

Nsengiyumva, et. al., (2015) examined the reliability and practicality of SCB test for evaluating the fracture characteristics of asphalt concrete mixtures. They investigated SCB for its repeatability for fracture test method by integrating a statistical experiment approach to identify testing variables of the SCB tests. After statistical analysis of 18 specimens with typical testing variables, it was found that five to six specimens were a reasonable sample size. They also investigated the sensitivity of the SCB test using the previously determined testing variables. Asphalt mixtures were collected from 12 field construction projects in Nebraska. They concluded that SCB test method is repeatable and sensitive to changes in the mixture and thus a promising tool for evaluating the fatigue fracture resistance of AC mixtures.

Saha & Biligiri, (2012) compiled the current knowledge about the utilization of SCB test to evaluate fracture properties of HMA. There was limited research regarding SCB test but still it was contemplated that the methodology of the test turns out to be a promising candidate to assess fracture performance. A review made by the authors presented the state-of-the-art utilization of SCB test to evaluate fracture properties of different asphalt mixtures. Furthermore, the study focused on the fundamental assessment of fractures through the static SCB test, which was based on load-deformation characteristics of asphalt mixes. Also, analytical solutions and application of fracture mechanics in evaluating fracture properties of asphalt mixes that led to the development of a standard monotonic SCB test protocol were discussed. Overall, dynamic SCB test procedure is a good crack propagation assessment in the areas of asphalt mix fracture characterization, Gedafa et. al. (2017).

2.3 Durability of Hot Mix Asphalt (HMA)

Durability of asphalt mixture is improved by additional asphalt binder content (Monismith, et. al. 1989). Additionally, it is enhanced by dense graded aggregate and uniformly compacted asphalt pavement. High asphalt content make asphalt protected against water because of its increased film thickness, and because of its increased average film thickness it decreases gap sizes between aggregates, thus making the mixture impenetrable to air and water (Monismith, et. al. 1989).

In 2015, Virginia Department of Transportation (VDOT) proposed changes to specifications of asphalt mix design. VDOT's proposal was to reduce design gyrations from 65 to 50 gyration. But, before modifications can be adopted Diefenderfer, et.al. (2018) performed a study to assess the effect the changes on mixture properties and lab performance. They evaluated eleven pairs of asphalt mix which consisted of typical specification of VDOT 65 gyration mix. Also, produced 50 gyration mix which was accorded to the proposed specification. They concluded that it had little effect on volumetric properties or gradations. Also, for the 50-gyration mixtures, core air voids were reduced, indicating the increase in durability of asphalt. Furthermore, because of increased asphalt binder, it resulted in an ability of the 50 gyration mixtures to be easily compacted in the field, which is expected to improve the durability of asphalt pavements in Virginia.

2.4 Effects of Asphalt Binder on Pavement Performance

2.4.1 Effect of N_{design} on Pavement Performance

An investigation of the effect of N_{design} values on performance of SuperPave mixtures was made in North Carolina. Qarouach, et. al. (2015) investigated surface mixes in NC with nominal aggregate sizes of 9.5mm and 12.5mm with various traffic levels. SuperPave design method was used to determine the asphalt content of each mixes. Asphalt pavement mixes were designed at N_{design} levels of 50, 75, 100, and 125. Asphalt Mixture Performance Tester (AMPT) device was utilized to measure optimum asphalt contents and dynamic modulus (E^*). Then, E^* data and binder properties were used as input in the AASHTO Darwin-ME software to predict rutting and fatigue performance of the asphalt mixtures. Then, relative performance recorded fatigue and rutting resistance for a specific mix was defined as the ratio of number of ESALs to failure for a given distress at a N_{design} level to the maximum ESALs (at 50 gyrations for fatigue and 125 gyrations for rutting). As they plotted the relative performance against asphalt content to determine optimum asphalt content, N_{design} was calculated as corresponding to the calculated optimum. Figure 7 illustrates the relative performance versus asphalt content.

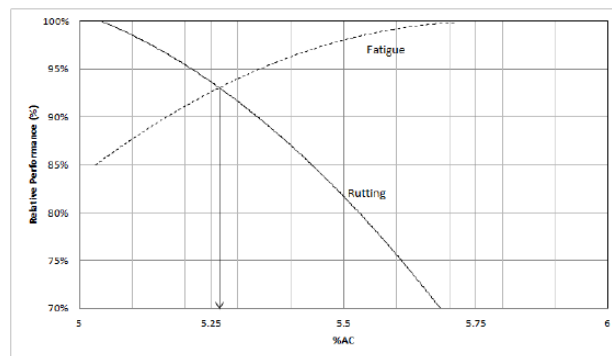


Figure 7. Relative Performance Versus Asphalt Content (Qarouach, et.al. 2015)

The number of gyrations for specific mixture is then determined from the plot of asphalt content vs gyrations as shown in Figure 8.

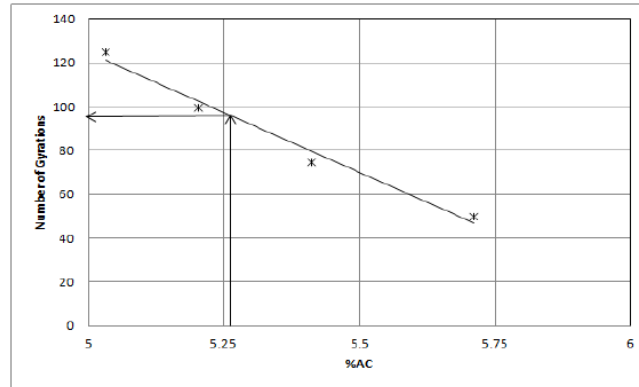


Figure 8. Number of Gyration Versus Asphalt Content (Qarouach, et.al. 2015)

Qarouach, et. al. (2015) observed that all the surface mixes with optimum asphalt content decreased with an increase in N_{design} level to which specimens were compacted. Also, mixtures stiffness is an extremely significant aspect of pavement design; it depends on the air void and asphalt contents of the mix and has effects on the fatigue performance of the pavement. Mixes with higher asphalt content binder exhibit lower fatigue cracking compared with lower asphalt content due to improved flexibility with excess asphalt binder. Furthermore, results from AMPT testing showed that the modulus of the mix at different temperature and frequencies increases with increase in N_{design} as observed from E^* master curves for each mix at various N_{design} levels. This only prove the theoretical basis of the study that using a higher N_{design} for mix design requires lower binder content and results in a stiffer mix. Finally, they developed their final recommendation from two primary recommendations:

- a. Effect of using a lower N_{design} on rutting and fatigue – improvement in pavement life with respect to fatigue life and corresponding increase in rutting (Qarouach, et. al. 2015).
- b. Effect of using higher N_{design} - economic benefits from reduced use of asphalt binder in the mix weighed against the reduction in fatigue life (Qarouach, et. al. 2015).

2.4.2 Rutting

Rutting in asphalt pavement is considered one of the major concerns in high temperature areas. Various research studies on rutting performance were made to mitigate the dilemma. There are two kinds of rutting, mix rutting and subgrade rutting (Washington Asphalt Pavement Association, 2010). Mix rutting is when the subgrade does not rut yet, but the pavement surface shows wheel path depressions from compaction or mix design problems. In contrast, subgrade rutting, occurs when the subgrade already has exhibited wheel path depressions due to vehicle loading, which makes the asphalt pavement more consolidated under the action of traffic (Pavement Interactive 2009; Ohio Asphalt, 2004). Hydroplaning is a phenomenon caused by ruts filled with water as vehicle skid resistance is reduced to near zero. It may be hazardous to drivers as it tends to pull a vehicle towards the rut path as it is steered across the rut which may cause vehicle collisions (Washington Asphalt Pavement Association 2010; Liley, 2018). Figure 9

shows that the pavement is displaced under the tires and humps up outside the wheel tracks. Users will not notice the depressions, but the depression will slowly pull the vehicle which may cause fatal injuries or accidents to users. Due to displacement under the tires, it will hump up outside the wheel tracks.

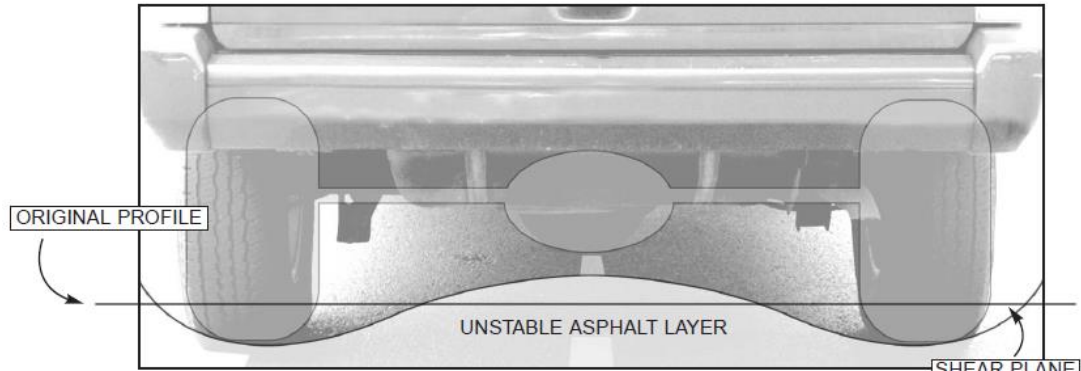


Figure 9. Asphalt Pavement Displaced Under the Tires (Ohio Asphalt, 2004)

Lack of compaction would be a probable cause of rutting in asphalt pavement. According to Liley (2018), one probable cause would be insufficient thickness of asphalt pavement and weak asphalt mixtures. Liley (2018) further explains that asphalt pavement requires specification that would be constructed in a way to prevent rutting and other distresses. Additionally, Ohio Asphalt (2004) added that a mix with low internal strength to resist deformations under loaded tires will experience rutting. Internal strength is affected by friction characteristics of the aggregates, especially the fine aggregate (Ohio Asphalt, 2004). This kind of distress has lots of various issues and it can be prevented by mixtures that are properly designed.

However, to reduce rutting failure to asphalt pavement, ruts can be investigated, and prevented. Ohio Asphalt (2004) claims that ruts can be prevented or reduced by maintaining a stiffer, stronger subbase. Subbase is explained to be important in the road system as it provides the support for which the road is built on. For construction of good quality rutting resistance pavement, strict quality control is a must. Also, providing good compaction by administering the proper weight, and number of passes of the roller over a section of asphalt plays a major role in ensuring the quality of the asphalt surface. Using angular aggregates tends to have higher internal friction that helps resist deformation under heavy loads (Ohio Asphalt, 2004). Liley (2018) argues that another way to combat rutting is to add more fine aggregate to increase its friction within the mix. Some suggestions would be using a global positioning system (GPS) or sensors in the roller to make sure that the roller can keep track of the number of passes. GPS or sensors can be utilized because the traditional method sometimes misses a section resulting in roads not receiving proper compaction.

Moghaddam et. al. (2011) reviewed and highlighted previous research works conducted on the effects of using different types of additives and aggregate gradation on rutting resistance of asphalt mixtures. It was observed that mixtures higher asphalt content affected the rutting performance of asphalt pavement. Furthermore, rutting properties of asphalt can be improved by adding different additives such as polymers and fibers as mentioned in their paper. Fibers and polymers can absorb a certain amount of distresses imposed by repetitive loading and may help postpone deteriorations such as rutting in asphalt pavements.

Maupin, et. al. (2003) investigated various laboratory test samples of the field mixes (12.5mm and 9.5mm) to predicted changes in mix properties as extra asphalt was added. They performed Rutting Test in accordance with VTM-110, Virginia Test Method for Determining Rutting Susceptibility using the APA. It was concluded that additional asphalt did not increase rutting for some mixes and decreased slightly for some when 1.0% asphalt was added, which did not appear to be a problem. It was an indication that mixes did not contain enough asphalt to decrease shear strength and substantially increase rutting. Furthermore, most mixes improved as the asphalt content was increased.

2.4.3 Fatigue Cracking.

There are several possible causes of fatigue cracking. Inadequate structural support, which can be caused by various issues like mix gradation problems. Decrease in pavement load supporting characteristics, like loss of base, subbase or subgrade support. Stripping at the bottom of the HMA layer, which contributes little to pavement strength so the effective HMA thickness decreases. Also, due to additional loads in traffic, asphalt pavement with poor construction and inadequate structural design, will fail and cause to crack and form alligator cracks on the surface (Washington Asphalt Pavement Association, 2010). As different problems may arise that will cause fatigue cracking, it is good practice to prevent or investigate the problem before the pavement loses its structural integrity.

Repair of fatigue cracking should be investigated to determine the cause of failure. Washington Asphalt Pavement Association (2010) explains that if an alligator pattern is demonstrated by the pavement, repair by crack sealing is ineffective. Investigation of the asphalt must be done comprising of digging a pit or coring in the asphalt pavement to determine the pavement's structural makeup as well if subsurface moisture is a factor. If the crack is small, it might be an indication of a loss of subgrade support. In contrast, if there is a huge crack, it is an indication of a general structural failure. HMA overlay that is structurally strong to carry heavy loads over the entire pavement surface is a solution. Prevention of fatigue cracking is attainable if the design and construction of asphalt pavement can support the expected traffic loads of a given highway.

Various studies about fatigue cracking performance were developed. Coleri et. al., (2018) characterized the cracking performance of asphalt pavements in Oregon by considering four (4) tests commonly used to evaluate fatigue cracking resistance. They proposed implementation of the most cost-effective and efficient test procedure for agencies and contractors. They concluded that SCB and IDT tests were the most practical and reliable tests that can be used to evaluate cracking resistance of asphalt mixtures. And that mixing method (laboratory or plant) does not have any significant effect on measured cracking performance. Binder content significantly affected the measured flexibility index (FI). A 0.7% increase in binder content raised the flexibility index by 2 to 3 times. They suggested that increasing binder content of asphalt mixtures currently used in the state can create significant savings and improve pavement longevity. Also, air-void content also significantly affected the measured FI. A 2% reduction in air-void content increases the flexibility index by 1.5 to 2 times. A higher flexibility index (FI) asphalt pavements may be more resistant to cracking and may increase longevity of asphalt pavements.

Maupin, et. al. (2003) additionally, investigated test samples for fatigue test included in the study from the previous section. Flexural beam fatigue test was performed in accordance with AASHTO Provisional Standard TP8-94, Standard Test Method for determining the fatigue

life of compacted hot mix asphalt subjected to repeated loading. The results for 12.5mm and 9.5mm mixes which has 7.4, 6.6, and 7.5 percent of asphalt content with an additional 0, 0.5, and 1.0 percent, respectively. The target voids were lower than the 7.5 percent attained for the beams containing 1.0 percent additional asphalt; therefore, they believed that the fatigue life would have been slightly higher with lower target voids. As a result of the slight increase in fatigue life when asphalt content was increased, it indicated that the improvement of fatigue life is not extensive when 0.5 percent asphalt is added.

Moghaddam, et al. (2011) included fatigue resistance for asphalt mixtures with different types of additives and aggregate gradation. It was observed that mixtures with higher asphalt content showed lower fatigue life. They also recommended that fatigue properties of asphalt can be improved by adding different additives such as polymers and fibers.

2.4.4 Low Temperature Cracking.

Transverse cracking can commence by single low temperature event or by multiple warming and cooling cycles and then multiply by further low temperature or traffic loadings (Minnesota Department of Transportation, 2014). Aschenbrener (1995) and Bradshaw (2016) studied that heavy snow and rain can cause the cracks to erode more aggressively over time, water can enter cracks and cause raveling of the joint and/or loss of base support. Investigation of thermal cracking is quantified by the frequency or spacing of the cracks and crack width (Aschenbrener, 1995). Due to thermal cracking, decrease in rideability of asphalt pavement is expected if not treated.

Testing of asphalt mixtures is important to accurately predict low temperature cracking performance of asphalt pavement in the field. Testing includes sophisticated techniques based on fracture mechanics rather than the current practice of stiffness and strength testing (Minnesota Department of Transportation, 2014). If cracks are left untreated for too long, they can lead to more problems and potentially more expensive repairs in the long run (Bradshaw, 2016). A research at Iowa revealed that cracks that were sealed properly were not as badly deteriorated as those which had not been sealed (Shelquist, et al. 1981). Thus, it was recommended by Aschenbrener (1995) that material properties can increase resistance of thermal cracking. Additionally, it was recommended by Shelquist, et al. (1981) that adopting a positive procedure requiring timely sealing of cracks is needed and strengthening specifications for preparing pavement surfaces for asphalt overlays is a must. Therefore, with pavement management and proper testing materials thermal cracks can be treated or prevented.

As the city of Pittsburgh uses SuperPave System for road pavement design consideration, Yeo, (2018) evaluated how to improve asphalt pavement in the city of Pittsburgh. It was mentioned in the study that thermal cracking and raveling increased as the asphalt aged. Pavement depth and the percentage of air voids in the pavement were important for the aging impacts of the asphalt pavement. Additionally, using the right performance grade (PG) of asphalt binder and aggregates were critical to prevent thermal cracking. It was recommended that in order to prevent thermal cracking in asphalt pavement, asphalt binder must be carefully selected, and it is crucial to study the right percentage of asphalt binder to be used in asphalt pavements in Pittsburgh.

A study on low temperature cracking was made by Li, et. al.(2007) in asphalt mixtures by using mechanical testing and acoustic emission methods. They investigated asphalt mixtures with the use of these methods to study microstructural phenomena and its corresponding effects on fracture behavior of asphalt mixtures at low temperatures. They tested eight asphalt mixtures,

which presented a combination of factors such as aggregate type, asphalt content, and air voids with the use of SCB tests at three low temperatures. It was concluded that fracture resistance was dependent on temperature and significantly affected by type of aggregate and air void content. They did not see any significant effect on fracture resistance from asphalt content.

Li & Marasteanu (2010) evaluated low temperature fracture resistance for asphalt mixes with the use of SCB test. They evaluated six asphalt mixtures, which represented various factors such as binder type, binder modifier, aggregate type, and air voids. Three replicates were evaluated, and results indicated strong dependence of the low temperature fracture resistance on the test temperature. As the fracture energy was calculated from the experimental data, result showed that fracture resistance of asphalt mixtures was affected by type of aggregate and air void content. They reported that the low limit of the binder PG grade has significant effect on the fracture resistance of asphalt mixture at low temperature. The results show that mixture with high PG grade 58 binder has higher fracture energy than mixture with high PG grade 64 binder. Although, PG 64 mixture was discovered to have greater peak load than the PG 58 mixture. So, it is consistent with the expectation that PG 58-28 binder is known “softer” than the PG 64-28 binder (Li & Marasteanu, 2010). They concluded that the mixture with PG58 binder is more resistant to cracking than PG64 binder.

Marasteanu et. al., (2007) investigated low temperature cracking in asphalt pavement. They had two sets of materials that were evaluated using the current testing specification such as the creep and strength for asphalt binders and mixtures as well as newly developed protocols, such as the DCT test, single edge notched beam test and SCB test. Dilatometric measurements were performed on both asphalt binder and mixtures to determine the coefficient of thermal contraction. Discrete fracture and damage tools were utilized in their research to model crack initiation and propagation in pavement systems using the finite element method and TCMODEL. These were used with the experimental data from the field samples to predict performance and compare it to the field performance data. They concluded that asphalt binder properties represent a key factor in designing asphalt mixtures resistant to low temperature cracking. However, the current asphalt binder testing does not provide enough reliability to predict low temperature cracking of asphalt pavements. Furthermore, aggregate type has a significant effect on the fracture properties of similar types of mixtures made with the same asphalt binder. Also, low temperature cracking is influenced by volumetric properties like specific gravity of the mix (G_{sb}) or theoretical maximum specific gravity (G_{mm}). The study clearly established that the effect of temperature is significant as the behavior changes from brittle-ductile to brittle, therefore, when doing low temperature tests on asphalt mixtures, testing temperatures should be established relative to the expected low pavement temperature and/or relative to the low temperature SuperPave Performance Grade (PG) for the location of interest.

3. METHODOLOGY

3.1 General

Blended aggregates that were used for the lab mixes were collected from North Dakota Department of Transportation. A total of four projects were selected for this research. Rutting, fatigue cracking and low-temperature cracking tests were done using Asphalt Pavement Analyzer (APA) Test, Semi-Circular Bending (SCB) Test, and Disc-Shaped Compact Tension (DCT) Test, respectively to develop the reduced N_{design} gyrations for the proposed project. The experimental plan for this research is summarized in Figure 11.

3.2 Project Selection

Four projects of different aggregate sources and binder grades were selected from North Dakota Department of Transportation projects. Two projects were selected from a high-volume highway class with Fine Aggregate Angularity (FAA) of 45 and binder grades 58H-28 and 58H-34, one project was selected from a medium volume highway class of FAA of 43 and binder grade of 58S-28, and one project was selected from a low volume highway class of FAA of 40 with binder grade of 58S-28. The gyratory compactive effort on the selected projects will be 75 gyrations, 65 gyrations, and either 55 or 50 gyrations. The low-end pavements with FAA of 43 and 40, where durability can be a concern, lower number of gyrations “50” was chosen. For high-end pavements with less durability concerns, a higher number of gyrations “55” was chosen. Table 2 shows the project number, binder type and HMA Grade provided by NDDOT.

Table 2 Project Summary

| Project Number | Location (Name) | Binder Type | Design Gyrations | HMA Grade |
|----------------------|---------------------|-------------|------------------|-----------|
| NH-TRP-3-002(160)213 | Devils Lake (Rugby) | 58H-28 | 75, 65, 55 | FAA 45 |
| NH-3-281(127)125 | New Rockford (Eddy) | 58H-34 | 75, 65, 55 | FAA 45 |
| IM-8-029(169)033 | Wahpeton (Fargo) | 58S-28 | 75, 65, 50 | FAA 40 |
| SS-6-032(060)164 | Grand Forks (GF) | 58S-28 | 75, 65, 50 | FAA 43 |

3.3 Mix Preparations and Computations

3.3.1 Mass Determination of Aggregate and Asphalt Binder.

Particle size distribution of aggregate sample is critical to obtain mix gradations in the lab similar to field gradations. After several experimental trials, it was decided to sieve the blended aggregate samples and determine batch weights to obtain accurate lab gradations. Tables 3,4, 5, and 6 show the distribution of batch weights of the four projects based on NDDOT Hot Mix Design Data and 6,000-gram aggregate samples.

Table 3. Rugby Mix Batch Weights

| Sieve Size | Batch Weights (g) | Batch Weights (%) |
|--------------------|-------------------|-------------------|
| +3/8 Material | 828.36 | 13.8 |
| -3/8, +#4 Material | 1311.6 | 21.9 |
| -#4 Material | 3860.04 | 64.3 |

Table 4. Eddy Mix Batch Weights

| Sieve Size | Batch Weights (g) | Batch Weights (%) |
|--------------------|-------------------|-------------------|
| +3/8 Material | 852.12 | 14.2 |
| -3/8, +#4 Material | 1,235.04 | 20.6 |
| -#4 Material | 3,912.84 | 65.2 |

Table 5. Fargo Mix Batch Weights

| Sieve Size | Batch Weights (g) | Batch Weights (%) |
|--------------------|-------------------|-------------------|
| +3/8 Material | 678.0 | 11.3 |
| -3/8, +#4 Material | 1134.0 | 18.9 |
| -#4 Material | 4188.0 | 69.8 |

Table 6. Grand Forks Mix Batch Weights

| Sieve Size | Batch Weights (g) | Batch Weights (%) |
|--------------------|-------------------|-------------------|
| +3/8 Material | 851.2 | 14.2 |
| -3/8, +#4 Material | 1650.8 | 27.5 |
| -#4 Material | 3498.0 | 58.3 |

Equation 1 was used to calculate the amount of asphalt binder in grams.

$$W_{ac} = \frac{W}{\left(\frac{100 - AC}{100}\right)} - W \quad (1)$$

Where:

- W = Total weight of aggregates in grams
- W_{ac} = Total weight of asphalt binder in grams
- AC = Asphalt Binder in percent (%)

3.3.2 Theoretical Maximum Specific Gravity (G_{mm}).

The theoretical maximum specific gravity (G_{mm}) of HMA is an experiment to determine the specific gravity of HMA excluding the air voids. Hence, to obtain the G_{mm} of a hot mix asphalt, air voids must be eliminated, and the combination of aggregate and asphalt binder would be the theoretical maximum specific gravity. In this research “Rice” density test procedure was utilized to determine the theoretical maximum specific gravity. Figure 10 shows the asphalt mix getting ready for theoretical maximum specific gravity experiment at room temperature. A total of 2000 grams of asphalt mix will be split into two samples and poured into the bowl together with water and the vacuum pump will be turned on and maintained at 25 mmHg for 15 minutes as seen in Figure 11. Figure 12 shows the usual set-up of the experiment.



Figure 10. Samples ready for Theoretical Maximum Specific Gravity (G_{mm}) testing



Figure 11. Set-up of bowl and Vacuum Gauge



Figure 12. Theoretical Maximum Specific Gravity (G_{mm}) Experiment Set-up

Due to the complexity of the value of G_{mm} which will be used to determine the air voids of compacted HMA, the standard procedure used was in accordance with AASHTO T209 to determine the theoretical maximum gravity of HMA. The typical values of theoretical maximum specific gravity of the mix ranges from 2.369 to 2.479 depending on the aggregate specific gravity and asphalt binder content. The theoretical maximum specific gravity of the mix was calculated from Equation 2.

$$G_{mm} = \frac{A}{(A + D - E)} \quad (2)$$

Where:

G_{mm} = Theoretical Maximum Specific Gravity of the mix

A = Sample mass in air (g)

D = Mass of bowl filled with water (g)

E = Mass of bowl and sample filled with water (g)

3.3.3 Mixing and Compaction of Asphalt Specimens.

SuperPave gyratory compactor (SGC) was used to compact specimens at the desired compaction levels. In this research, 75, 65, 55 and 50 gyrations were used to determine the optimal asphalt content for a specified gyration. Following the AASHTO T312, lab mix aggregates were heated for 12 to 24 hours at a temperature of 325 °F and asphalt binder was heated at 290 °F for 3 to 4 hours. Also, mixing bowls, trays, asphalt spoons and wire whips were heated in the same oven as the asphalt binder at the same temperature (290 °F). When all the materials, aggregates and asphalt binder were ready, asphalt binder and aggregate were mixed using asphalt bowls and wire whisk as shown in Figure 13, and they were brought in an oven and short term aged for two hours at a temperature of 280 °F. When the asphalt is ready after two hours, mix will be inserted in the SGC machine as seen on Figure 14.



Figure 13. Mixing Bowls and Wire Whisks



Figure 14. SuperPave Gyrotory Compactor

While the hot mixed asphalt was heated in the oven, the molds, transfer pan, asphalt spoons were heated in a different oven at the same time. Additionally, the SuperPave gyrotory compactor was prepared and calibrated to 600 kPa.

After 2 hours of short-term aging of hot mix asphalt, the tray of asphalt mix was moved to a transfer pan and the mix was placed in the compaction mold. As the mold with asphalt mix was charged, the external angle was set to $1.25^\circ \pm 0.03^\circ$ and with an internal angle of $1.16^\circ \pm 0.03^\circ$. After the desired compaction level (75, 65, 55 or 50) is achieved, the gyrotory compactor

automatically stops, and asphalt plugs are ready for determination of bulk specific gravity (G_{mb}) and percent air-voids.

3.3.4 Bulk Specific Gravity of the Mix (G_{mb}).

After the asphalt plugs were compacted, they were prepared for the determination of bulk specific gravity of the mix. For the preparation of this experiment, AASHTO T-166 was followed. Equation 3 below was used to determine G_{mb} .

$$G_{mb} = \frac{A}{B - C} \quad (3)$$

Where:

- G_{mb} = Bulk Specific Gravity of the mix
- A = mass of sample in air (g)
- B = mass of SSD sample in air (g)
- C = mass of sample in water (g)

There are different procedures under AASHTO T 166. In this research, saturated surface dry (SSD) was the method used. The SSD is the most common method that calculates the specimen volume by subtracting the mass of the specimen under water from the mass of an SSD specimen. To get the following parameters, mass of sample in air was determined with a calibrated scale. After recording the mass of sample in air, the asphalt plug was submerged in water with a temperature of 25°C (77°F) for 4 minutes as seen in Figure 15. Then, after recording the mass of sample in water, the asphalt plug must be quickly dried with a damp towel and the surface dry mass of the sample would be recorded. The typical values of bulk specific gravity of mixture ranges from 2.202 to 2.328 depending upon the bulk specific gravity of the aggregate, the asphalt binder content, and amount of compaction. Figure 16 shows the prepared compacted asphalt mix samples for G_{mb} testing.



Figure 15. Sample Asphalt Plug Weighed in Air and Sample Submerged Under Water



Figure 16. Asphalt Samples Ready for G_{sb} Experiment

3.3.5 Percent (%) Air Voids of the Specimen (V_a).

Once G_{mm} and G_{mb} are known, percent air voids can be calculated. It is calculated by comparing G_{mb} and G_{mm} and quantified as a percentage. Through the determination of air voids, it is assumed that the difference of both values is due to air. The computation to obtain the percent air voids is calculated with Equation 4.

$$AV = \left(\frac{G_{mm} - G_{mb}}{G_{mm}} \right) \times 100\% \quad (4)$$

Where:

- AV = Air Voids (%)
- G_{mm} = Theoretical Maximum Specific Gravity of the Mix
- G_{mb} = Bulk Specific Gravity of the Mix

3.4 Performance Testing

Rutting, low temperature cracking, and fatigue cracking were determined using Asphalt Pavement Analyzer (APA), Semi-Circular Bend (SCB) Test and Disk-shaped Compaction Tension (DCT) Test, respectively. All the asphalt plugs must meet the $7.0 \pm 1.0\%$ air void content criteria to mimic constructed asphalt pavements. Figure 17 shows the machines used to prepare sample specimens.



Figure 17. Cutting, Drilling and Sawing Machines

3.4.1 APA Test.

Asphalt Pavement Analyzer was utilized to determine the rutting performance following AASHTO T340. The APA is a temperature-controlled wheel tracking device. The machine measures the rutting that develops from laboratory compacted specimens. The APA features controllable wheel load and contact pressure that represents actual field conditions. The SGC was used to compact the cylindrical specimens that are 6 inches (150mm) in diameter and 3 inches (75mm) in height that was in accordance with AASHTO T 340. Rutting in the asphalt specimens was induced with the use of pressurized hoses to 100 psi and placed over the compacted asphalt specimens. Samples were conditioned for 5 to 6 hours in the APA cabin at 58°C prior to APA testing, and after 8,000 cycles, rut depths are recorded. In analyzing the results, APA performance specification is based on the evaluation of rutting performance mixes from North Dakota mixes that has an average of 7mm, 8mm, or 9mm rut depth for high-class, middle-class, and low-class pavements, respectively (Suleiman, 2005).

3.4.2 DCT Test.

Disk-Shaped Compact Tension test was utilized to determine the fracture energy of lab compacted specimens following ASTM D7313. The DCT is used as performance-type test specification to control different forms of cracking, such as thermal, reflective, and block cracking of pavements surfaced with asphalt pavement. Sample specimens were conditioned for 8 hours at low temperature PG+10°C of the binder. During the test, a constant Crack Mouth Opening Displacement (CMOD) rate of 0.017 mm/s was maintained.

Disk Shaped specimen is pulled apart until the post peak level has generated to 0.02 lb (0.1 kN). As for the geometry of the specimen, it has a 6-inch (150mm) diameter, 2-inch (50mm) thick overall dimension with two 1-inch (25mm) holes on either side of a 2.46-inch (62.5-mm) notch cut into a flattened portion of the circumference as shown in Figure 18. Figure 19 shows the typical set-up of DCT test.



Figure 18. DCT Samples Ready for Testing



Figure 19. DCT Sample Set-Up

Fracture energy (G_f) is calculated by determining the area under the load, CMOD curve normalized the initial ligament length and thickness. The larger the G_f , the better the cracking resistance of the asphalt mixture is. The typical coefficient of variation (COV) for the DCT test for virgin mixtures is around 10 percent. Figure 20 displays a sample graph of CMOD versus Load (kN).

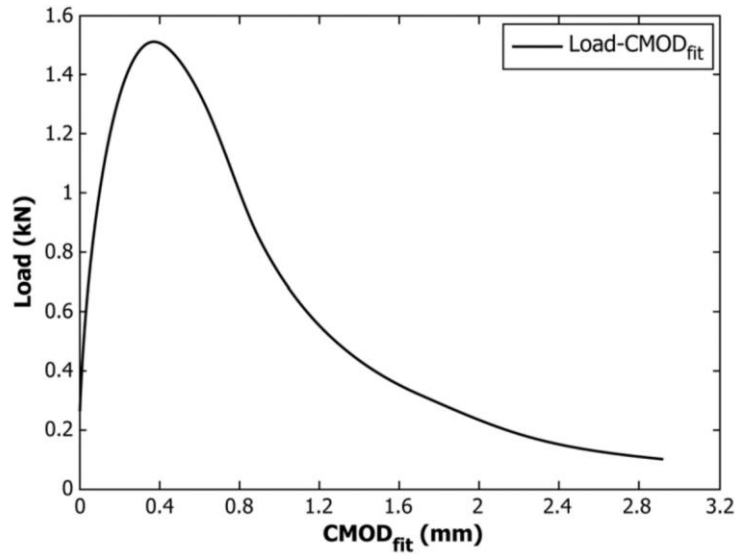


Figure 20. Typical Load vs CMOD_{fit}

3.4.3 SCB Test.

Fatigue resistance was determined in accordance with AASHTO TP124-16. Illinois-Flexibility Index Tester (IFIT) protocol was used for samples with sizes of 50±2mm and were tested using the SCB to determine fatigue cracking resistance of laboratory compacted samples. The samples were conditioned for 2 hours and tested at 25°C. Fracture energy is the total area under load vs displacement curve and FI is the slope of the curve post peak load. FI was calculated using Equation 5. Figure 21 shows typical asphalt samples ready for testing. Figure 22 displays the typical set-up for an SCB test. Typical load vs displacement is shown in figure 23.

$$FI = \frac{Gf}{|m|} \times A \quad (5)$$

Where:

FI = Flexibility Index

Gf = Fracture Energy (J/m²)

$|m|$ = Absolute value of post – peak load slope (kN/mm)

A = conversion factor = 0.01



Figure 21. SCB Samples Ready for Testing

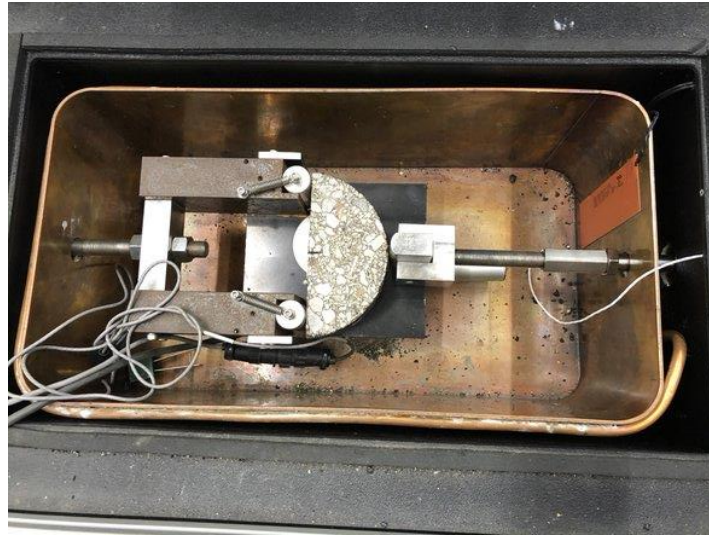


Figure 22. SCB Sample Set-Up

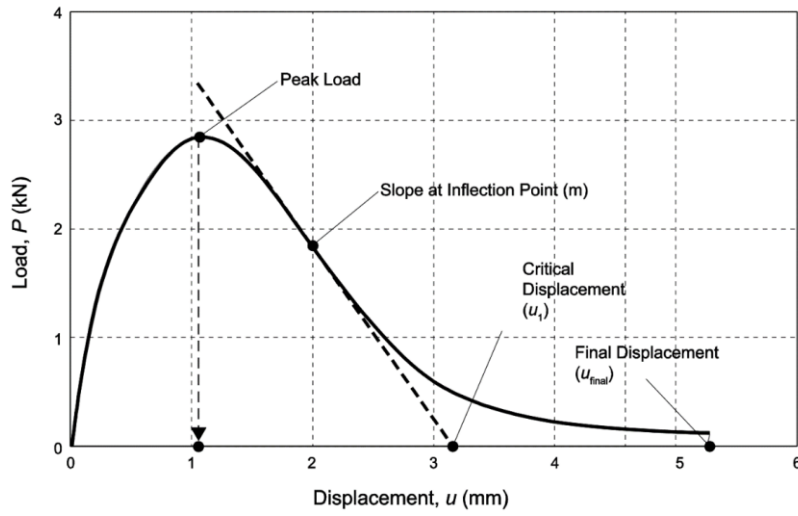


Figure 23. Typical Load Vs Displacement

4. RESULTS AND DISCUSSIONS

4.1 Theoretical Maximum Specific Gravity

The maximum theoretical specific gravity values for all the projects were obtained using the AASHTO T209 procedure. G_{mm} results for the Rugby, Eddy, Fargo, and Grand Forks project mixes are reported in Tables 7, 8, 9, and 10.

Table 7. G_{mm} Results for Rugby Mix

| Asphalt Content (%) | Sample Mass in Air in grams (A) | Mass of Bowl Filled with Water in grams (D) | Mass of Bowl Filled with Water and Asphalt in grams (E) | G_{mm} Results | G_{mm} Average |
|---------------------|---------------------------------|---|---|------------------|------------------|
| 5.0 | | | | | |
| Bowl 1 | 750.3 | 7566.6 | 8018.8 | 2.517 | |
| Bowl 2 | 750.3 | 7566.6 | 8018.9 | 2.518 | 2.517 |
| | | | Tolerance | 0.001 | |
| 5.5 | | | | | |
| Bowl 1 | 750.4 | 7564.6 | 8013.5 | 2.489 | |
| Bowl 2 | 750.3 | 7564.6 | 8013 | 2.485 | 2.487 |
| | | | Tolerance | 0.004 | |
| 6.0 | | | | | |
| Bowl 1 | 750.5 | 7566.6 | 8012.3 | 2.462 | |
| Bowl 2 | 750.5 | 7566.6 | 8011.5 | 2.456 | 2.459 |
| | | | Tolerance | 0.006 | |
| 6.5 | | | | | |
| Bowl 1 | 750.4 | 7566.6 | 8009.6 | 2.441 | |
| Bowl 2 | 750.3 | 7566.6 | 8008.3 | 2.431 | 2.436 |
| | | | Tolerance | 0.010 | |
| 7.0 | | | | | |
| Bowl 1 | 750.1 | 7566.6 | 8006.3 | 2.417 | |
| Bowl 2 | 750.6 | 7566.6 | 8007.5 | 2.424 | 2.420 |
| | | | Tolerance | 0.007 | |

Table 8. G_{mm} Results for Eddy Mix

| Asphalt Content (%) | Sample Mass in Air in grams (A) | Mass of Bowl Filled with Water in grams (D) | Mass of Bowl Filled with Water and Asphalt in grams (E) | G_{mm} Results | G_{mm} Average |
|---------------------|---------------------------------|---|---|------------------|------------------|
| 5.0 | | | | | |
| Bowl 1 | 750.6 | 7566.6 | 8016.7 | 2.498 | |
| Bowl 2 | 750.9 | 7566.6 | 8017.5 | 2.503 | 2.500 |
| | | | Tolerance | 0.005 | |
| 5.5 | | | | | |
| Bowl 1 | 750.1 | 7566.6 | 8015.1 | 2.487 | |

| | | | | | |
|--------|-------|--------|-----------|-------|--------------|
| Bowl 2 | 750.4 | 7566.6 | 8014.1 | 2.477 | 2.482 |
| | | | Tolerance | 0.010 | |
| 6.0 | | | | | |
| Bowl 1 | 750.2 | 7566.6 | 8012.2 | 2.463 | |
| Bowl 2 | 750.4 | 7566.6 | 8013.4 | 2.472 | 2.467 |
| | | | Tolerance | 0.009 | |
| 6.5 | | | | | |
| Bowl 1 | 750.3 | 7566.6 | 8012.2 | 2.462 | |
| Bowl 2 | 750.4 | 7566.6 | 8011.3 | 2.455 | 2.459 |
| | | | Tolerance | 0.008 | |
| 7.0 | | | | | |
| Bowl 1 | 750.4 | 7566.6 | 8010.5 | 2.448 | |
| Bowl 2 | 750.5 | 7566.6 | 8009.6 | 2.441 | 2.444 |
| | | | Tolerance | 0.008 | |

Table 9. G_{mm} Results for Fargo Mix

| Asphalt Content (%) | Sample Mass in Air in grams (A) | Mass of Bowl Filled with Water in grams (D) | Mass of Bowl Filled with Water and Asphalt in grams (E) | G_{mm} Results | G_{mm} Average |
|---------------------|---------------------------------|---|---|------------------|------------------|
| 5.0 | | | | | |
| Bowl 1 | 750.7 | 7566.6 | 8015.3 | 2.486 | |
| Bowl 2 | 750.5 | 7566.9 | 8014.8 | 2.480 | 2.483 |
| | | | Tolerance | 0.006 | |
| 5.5 | | | | | |
| Bowl 1 | 750.5 | 7566.6 | 8012.3 | 2.462 | |
| Bowl 2 | 750.8 | 7566.6 | 8013.3 | 2.469 | 2.466 |
| | | | Tolerance | 0.007 | |
| 6.0 | | | | | |
| Bowl 1 | 750.7 | 7566.6 | 8011.2 | 2.452 | |
| Bowl 2 | 750.2 | 7566.6 | 8010.6 | 2.450 | 2.451 |
| | | | Tolerance | 0.002 | |
| 6.5 | | | | | |
| Bowl 1 | 750.4 | 7566.6 | 8008.8 | 2.435 | |
| Bowl 2 | 750.3 | 7566.6 | 8009 | 2.437 | 2.436 |
| | | | Tolerance | 0.002 | |
| 7.0 | | | | | |
| Bowl 1 | 750.2 | 7566.6 | 8008.6 | 2.434 | |
| Bowl 2 | 750.7 | 7566.6 | 8007.2 | 2.421 | 2.427 |
| | | | Tolerance | 0.013 | |

Table 10. G_{mm} Results for Grand Forks Mix

| Asphalt Content (%) | Sample Mass in Air in grams (A) | Mass of Bowl Filled with Water in grams (D) | Mass of Bowl Filled with Water and Asphalt in grams (E) | G_{mm} Results | G_{mm} Average |
|---------------------|---------------------------------|---|---|------------------|------------------|
| 5.5 | | | | | |
| Bowl 1 | 975.3 | 7559.4 | 8152.6 | 2.552 | |
| Bowl 2 | 973.4 | 7560.2 | 8151.9 | 2.550 | 2.551 |
| | | | Tolerance | 0.002 | |
| 6.0 | | | | | |
| Bowl 1 | 1030.1 | 7559.4 | 8175.3 | 2.487 | |
| Bowl 2 | 1030.4 | 7560.2 | 8174.6 | 2.477 | 2.482 |
| | | | Tolerance | 0.010 | |
| 6.5 | | | | | |
| Bowl 1 | 1013.2 | 7559.4 | 8157.1 | 2.439 | |
| Bowl 2 | 1013.6 | 7560.2 | 8157.2 | 2.433 | 2.436 |
| | | | Tolerance | 0.005 | |
| 7.0 | | | | | |
| Bowl 1 | 1016.4 | 7559.4 | 8155.8 | 2.420 | |
| Bowl 2 | 1020.5 | 7560.2 | 8157.9 | 2.414 | 2.417 |
| | | | Tolerance | 0.006 | |
| 7.5 | | | | | |
| Bowl 1 | 1021.3 | 7559.4 | 8154.7 | 2.397 | |
| Bowl 2 | 1220.2 | 7560.2 | 8268.8 | 2.385 | 2.391 |
| | | | Tolerance | 0.012 | |
| 8.0 | | | | | |
| Bowl 1 | 1073.3 | 7559.4 | 8180.2 | 2.372 | |
| Bowl 2 | 1086 | 7560.2 | 8187.8 | 2.369 | 2.371 |
| | | | Tolerance | 0.003 | |
| 8.5 | | | | | |
| Bowl 1 | 1045.8 | 7559.4 | 8163.1 | 2.366 | |
| Bowl 2 | 1040.7 | 7560.2 | 8162.4 | 2.373 | 2.369 |
| | | | Tolerance | 0.008 | |

It should be noted here that the G_{mm} values for Rugby, Eddy, and Fargo mixes were determined by the graduate student. He only used bowl # 1 for the calculations. For the Grand Forks mix, the PI determined the G_{mm} results and used bowls 1 and 2 with slightly different values. A summary of G_{mm} results for all the mixes with comparison with NDDOT mix design values are shown in Table 11. The G_{mm} results are slightly different from NDDOT mix design G_{mm} values as expected due to sampling considerations.

Table 11. UND Lab G_{mm} Results VS NDDOT Mix Design Values

| Project Number | AC Binder | AC (%) | G_{mm} Values | |
|----------------------|-----------|--------|------------------|-------------|
| | | | NDDOT Mix Design | UND Lab Mix |
| Rugby | | | | |
| NH-TRP-3-002(160)213 | 58H -28 | 5.0 | 2.500 | 2.517 |
| | 58H -28 | 5.5 | 2.481 | 2.487 |
| | 58H -28 | 6.0 | 2.466 | 2.459 |
| | 58H -28 | 6.5 | 2.451 | 2.436 |
| | 58H -28 | 7.0 | - | 2.420 |
| Eddy | | | | |
| NH-3-281(127)125 | 58H - 34 | 4.5 | 2.514 | - |
| | 58H - 34 | 5.0 | 2.492 | 2.500 |
| | 58H - 34 | 5.5 | 2.472 | 2.482 |
| | 58H - 34 | 6.0 | 2.456 | 2.467 |
| | 58H - 34 | 6.5 | - | 2.459 |
| | 58H - 34 | 7.0 | - | 2.444 |
| Fargo | | | | |
| IM-8-029(169)033 | 58S - 28 | 5.0 | 2.495 | 2.483 |
| | 58S - 28 | 5.5 | 2.473 | 2.466 |
| | 58S - 28 | 6.0 | 2.451 | 2.451 |
| | 58S - 28 | 6.5 | 2.430 | 2.436 |
| | 58S - 28 | 7.0 | - | 2.427 |
| Grand Forks | | | | |
| SS-6-032(060)164 | 58S - 28 | 5.5 | 2.441 | 2.551 |
| | 58S - 28 | 6.0 | 2.428 | 2.482 |
| | 58S - 28 | 6.5 | 2.406 | 2.436 |
| | 58S - 28 | 7.0 | 2.383 | 2.417 |
| | 58S - 28 | 7.5 | - | 2.391 |
| | 58S - 28 | 8.0 | - | 2.371 |
| | 58S - 28 | 8.5 | - | 2.369 |

4.2 Determination of Optimum Asphalt Content

Optimum asphalt content was determined by accomplishing relating air voids and binder content linear graph. The best fit line was utilized to determine the required asphalt content at 4% air voids. The linear equation in each graph was used to obtain the asphalt content at 4% air voids which is required by NDDOT. Seventy-five, 65, and 55 gyrations were applied to the SGC to determine the optimum asphalt content on their respective compaction effort for the Rugby and Eddy mixes. Additionally, 75, 65, and 50 gyrations were applied to the SGC to determine the optimum asphalt content on their respective compaction effort for the Fargo and Grand Forks mixes. Tables 12, 13, and 14 as well as Figures 24, 25, and 26 display the G_{mb} calculations for the Rugby mix at 75, 65, and 55 gyrations, respectively. In an effort to save scarce aggregate and binder materials, binder content calculations for 65 and 55 gyrations were interpreted from two-point binder content calculations.

Table 12. Air Voids Calculations VS Asphalt Contents at 75 Gyration (Rugby)

| Asphalt Content (%) | Gmb | Gmm | Air Voids (%) |
|---------------------|-------|-------|---------------|
| 5.0 | 2.321 | 2.517 | 7.82 |
| 5.5 | 2.368 | 2.487 | 4.80 |
| 6.0 | 2.374 | 2.459 | 3.45 |
| 6.5 | 2.383 | 2.436 | 2.20 |

Table 13. Air Voids Calculations VS Asphalt Contents at 65 Gyration (Rugby)

| Asphalt Content (%) | Gmb | Gmm | Air Voids % |
|---------------------|-------|-------|-------------|
| 6.0 | 2.348 | 2.459 | 4.53 |
| 6.5 | 2.383 | 2.436 | 2.20 |

Table 14. Air Voids Calculations VS Asphalt Contents at 55 Gyration (Rugby)

| Asphalt Content (%) | Gmb | Gmm | Air Voids % |
|---------------------|-------|-------|-------------|
| 6.5 | 2.330 | 2.436 | 4.37 |
| 7.0 | 2.351 | 2.420 | 2.86 |

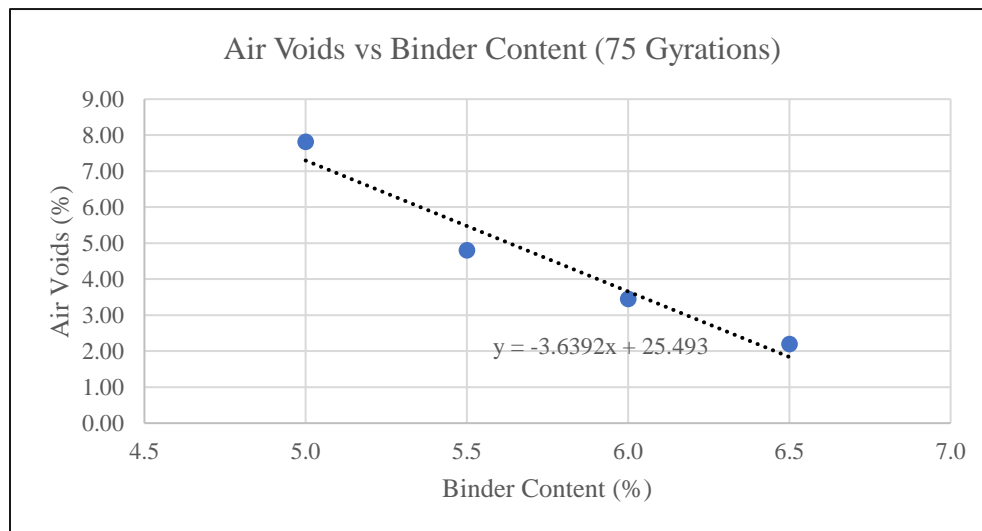


Figure 24. Air Voids vs Binder Content (75 Gyration) – Rugby Mix

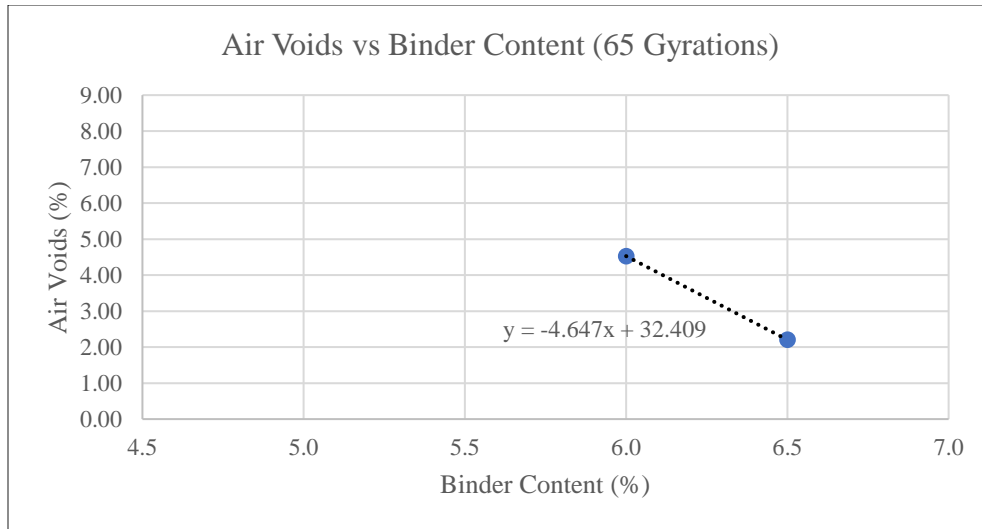


Figure 25. Air Voids vs Binder Content at 65 Gyration – Rugby Mix

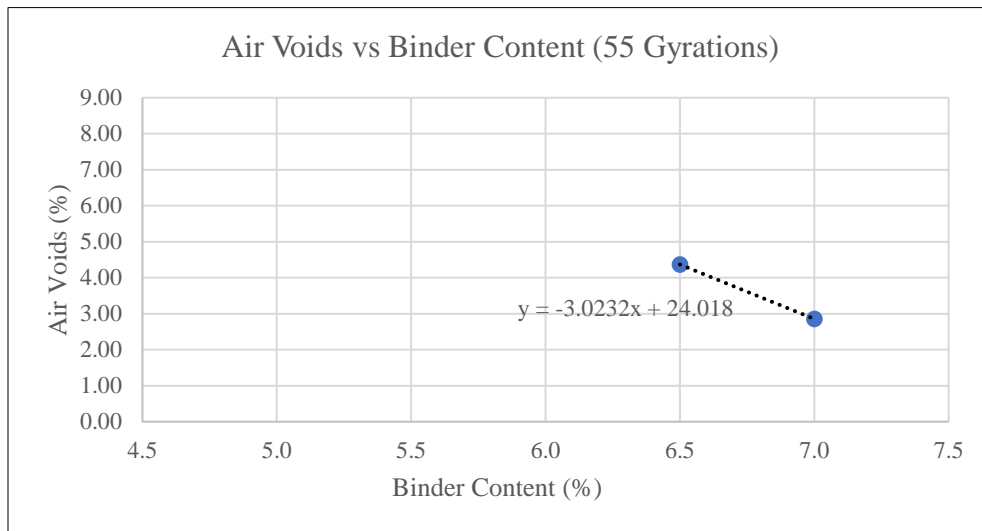


Figure 26. Air Voids vs Binder Content at 55 Gyration – Rugby Mix

Similar to Rugby project, binder content calculations for Eddy, Fargo, and Grand Forks mixes for the different gyration levels were determined and displayed in tables 15 through 23 and figures 27 through 35.

Table 15. Air Voids Calculations VS Asphalt Contents at 75 Gyration (Eddy)

| Asphalt Content (%) | Gmb | Gmm | Air Voids (%) |
|---------------------|-------|-------|---------------|
| 5.0 | 2.368 | 2.500 | 5.28 |
| 5.5 | 2.374 | 2.482 | 4.37 |
| 6.0 | 2.388 | 2.467 | 3.22 |
| 6.5 | 2.406 | 2.459 | 2.14 |

Table 16. Air Voids Calculations VS Asphalt Contents at 65 Gyration (Eddy)

| Asphalt Content (%) | Gmb | Gmm | Air Voids (%) |
|---------------------|-------|-------|---------------|
| 6.0 | 2.363 | 2.467 | 4.21 |
| 6.5 | 2.396 | 2.459 | 2.56 |

Table 17. Air Voids Calculations VS Asphalt Contents at 55 Gyration (Eddy)

| Asphalt Content (%) | Gmb | Gmm | Air Voids (%) |
|---------------------|-------|-------|---------------|
| 6.5 | 2.353 | 2.459 | 4.28 |
| 7.0 | 2.368 | 2.444 | 3.12 |

Table 18. Air Voids Calculations VS Asphalt Contents at 75 Gyration (Fargo)

| Asphalt Content (%) | Gmb | Gmm | Air Voids (%) |
|---------------------|-------|-------|---------------|
| 5.0 | 2.311 | 2.483 | 6.91 |
| 5.5 | 2.347 | 2.466 | 4.82 |
| 6.0 | 2.395 | 2.451 | 2.28 |
| 6.5 | 2.400 | 2.436 | 1.48 |

Table 19. Air Voids Calculations VS Asphalt Contents at 65 Gyration (Fargo)

| Asphalt Content (%) | Gmb | Gmm | Air Voids (%) |
|---------------------|-------|-------|---------------|
| 5.5 | 2.279 | 2.466 | 7.56 |
| 6.0 | 2.330 | 2.451 | 4.94 |
| 6.5 | 2.401 | 2.436 | 1.45 |

Table 20. Air Voids Calculations VS Asphalt Contents at 50 Gyration (Fargo)

| Asphalt Content (%) | Gmb | Gmm | Air Voids (%) |
|---------------------|-------|-------|---------------|
| 6.0 | 2.282 | 2.451 | 6.89 |
| 6.5 | 2.313 | 2.436 | 5.05 |
| 7.0 | 2.352 | 2.427 | 3.10 |

Table 21. Air Voids Calculations VS Asphalt Contents at 75 Gyration (GF)

| Asphalt Content (%) | Gmb | Gmm | Air Voids (%) |
|---------------------|-------|-------|---------------|
| 5.5 | 2.235 | 2.551 | 12.38 |
| 6.0 | 2.250 | 2.482 | 9.33 |
| 6.5 | 2.277 | 2.436 | 6.52 |
| 7.0 | 2.300 | 2.417 | 4.84 |
| 7.5 | 2.321 | 2.391 | 2.92 |

Table 22. Air Voids Calculations VS Asphalt Contents at 65 Gyration (GF)

| Asphalt Content (%) | Gmb | Gmm | Air Voids (%) |
|---------------------|-------|-------|---------------|
| 7.0 | 2.235 | 2.417 | 7.53 |
| 7.5 | 2.237 | 2.391 | 6.45 |
| 8.0 | 2.322 | 2.371 | 2.08 |

Table 23. Air Voids Calculations VS Asphalt Contents at 50 Gyration (GF)

| Asphalt Content | Gmb | Gmm | Air Voids % |
|-----------------|-------|-------|-------------|
| 7.5 | 2.238 | 2.391 | 6.40 |
| 8.0 | 2.273 | 2.371 | 4.13 |
| 8.5 | 2.281 | 2.369 | 3.71 |

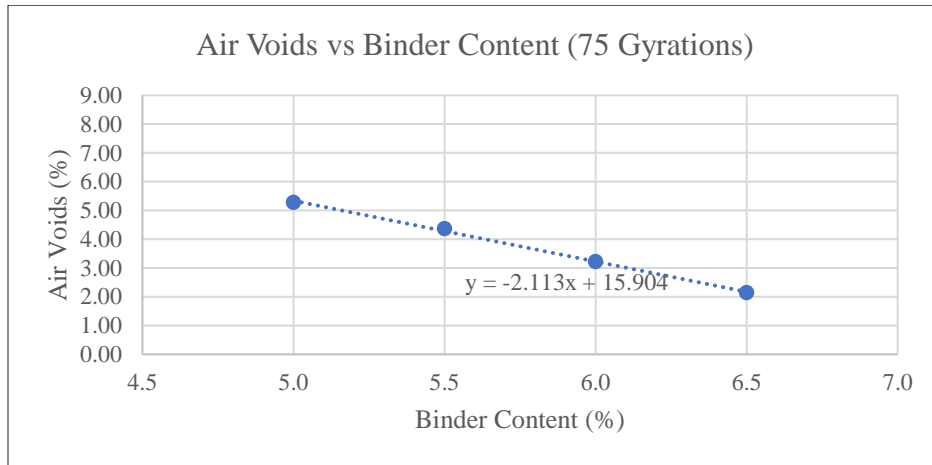


Figure 27. Air Voids vs Binder Content at 75 Gyration – Eddy Mix

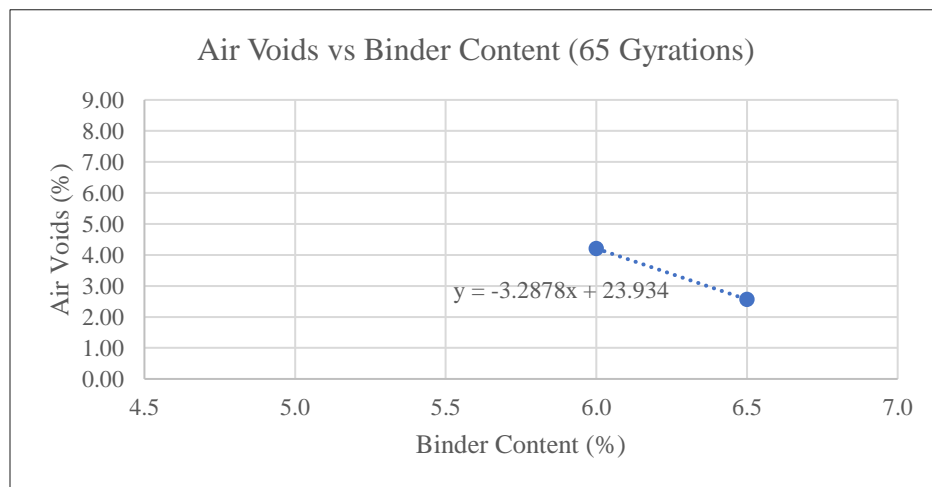


Figure 28. Air Voids vs Binder Content at 65 Gyration – Eddy Mix

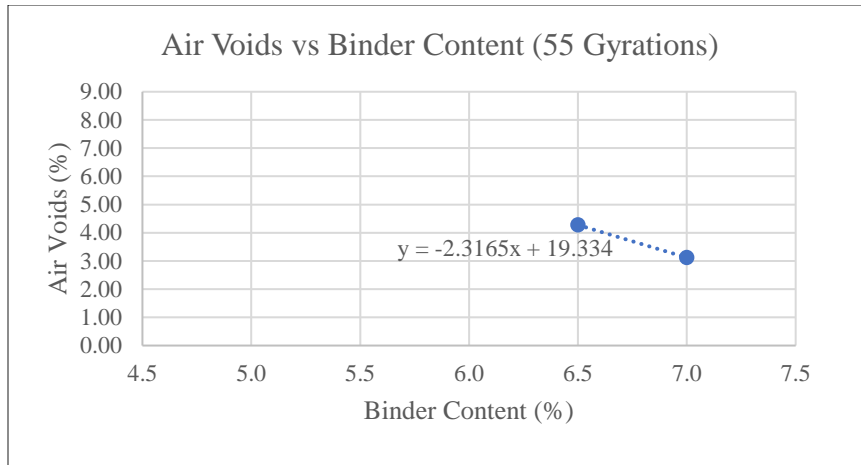


Figure 29. Air Voids vs Binder Content at 55 Gyration – Eddy Mix

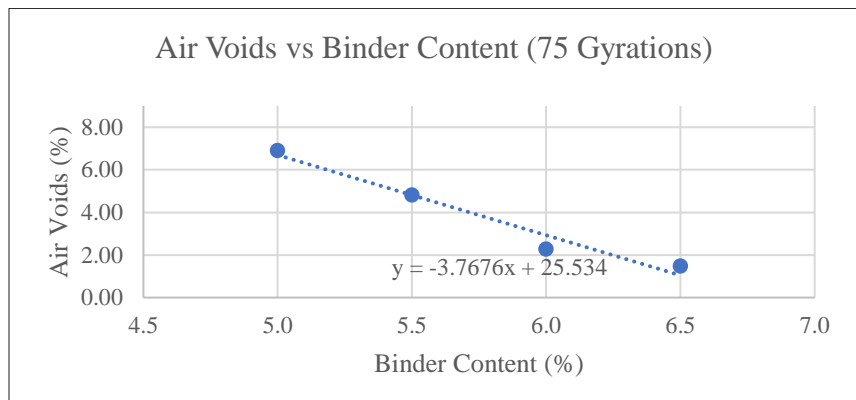


Figure 30. Air Voids vs Binder Content at 75 Gyration – Fargo Mix

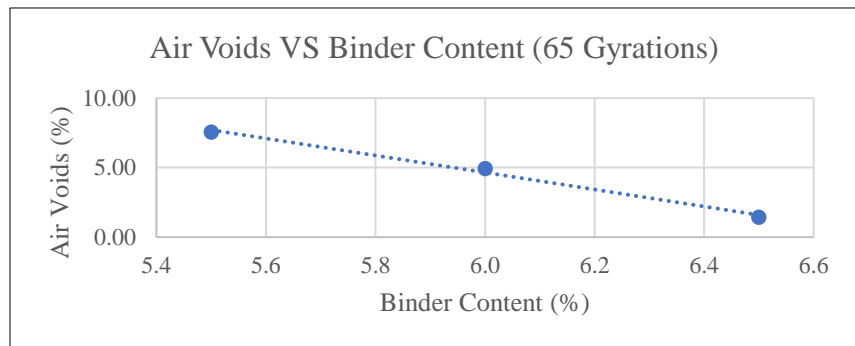


Figure 31. Air Voids vs Binder Content at 65 Gyration – Fargo Mix

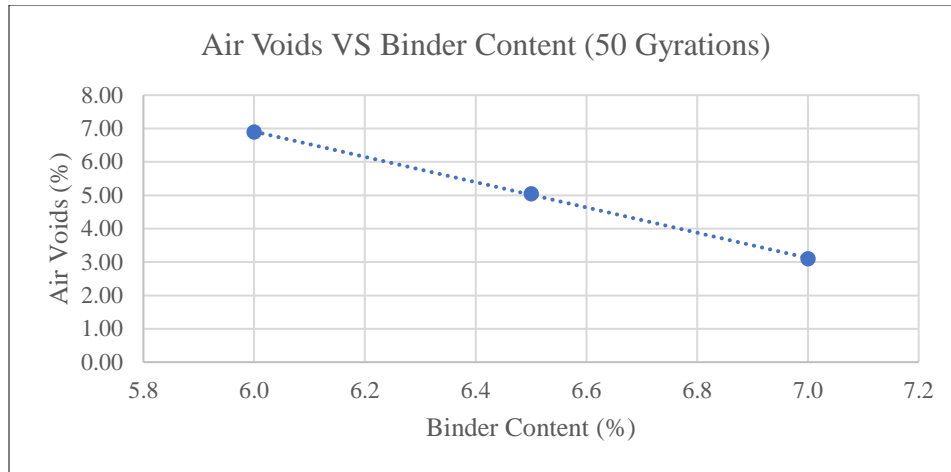


Figure 32. Air Voids vs Binder Content at 50 Gyration – Fargo Mix

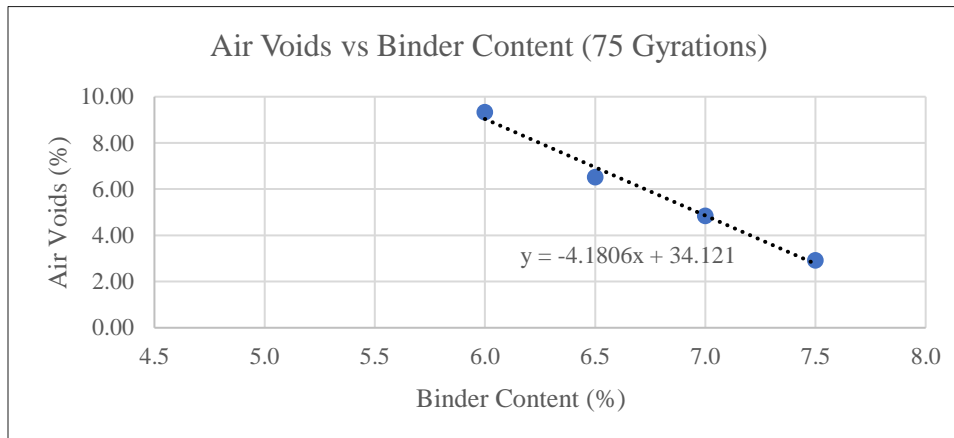


Figure 33. Air Voids vs Binder Content at 75 Gyration – GF Mix

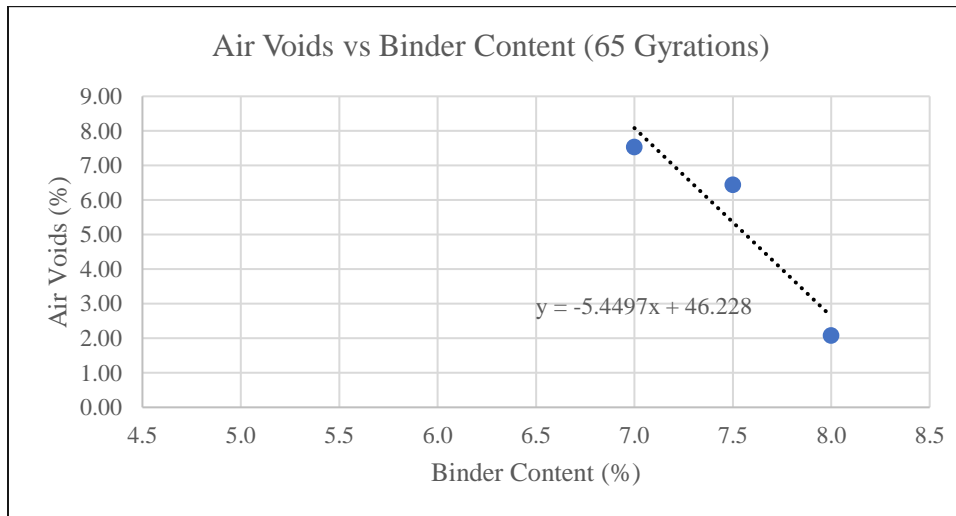


Figure 34. Air Voids vs Binder Content at 65 Gyration – GF Mix

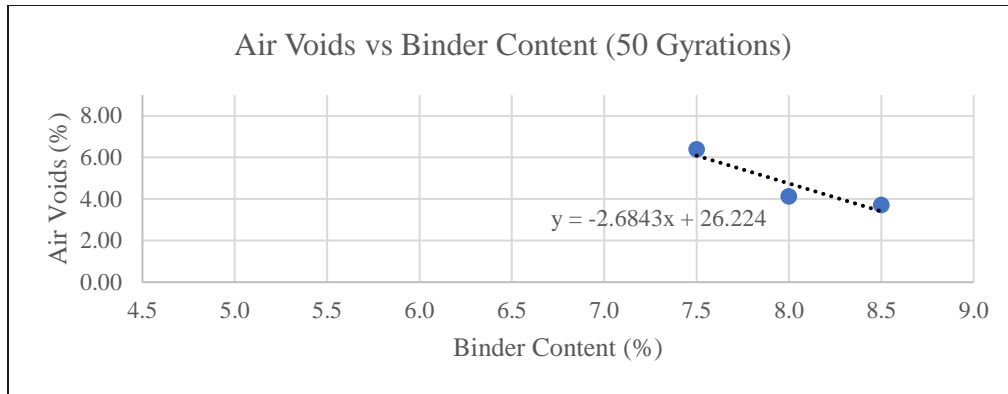


Figure 35. Air Voids vs Binder Content at 50 Gyration – GF Mix

The summary optimal binder content results of all project mixes and gyration levels are displayed in Table 24. G_{mm} values at optimal asphalt content for all the projects are also displayed in Table 24.

Table 24. Optimal Binder Content and G_{mm} Values for All mixes and Gyration Levels

| | Optimal Binder Content | G_{mm} at Optimal Binder Content |
|--------------------|-------------------------------|--|
| Rugby | | |
| 75 Gyration | 5.90% | 2.456 |
| 65 Gyration | 6.10% | 2.454 |
| 55 Gyration | 6.60% | 2.433 |
| Eddy | | |
| 75 Gyration | 5.60% | 2.479 |
| 65 Gyration | 6.10% | 2.465 |
| 55 Gyration | 6.60% | 2.456 |
| Fargo | | |
| 75 Gyration | 5.70% | 2.460 |
| 65 Gyration | 6.10% | 2.448 |
| 50 Gyration | 6.70% | 2.432 |
| Grand Forks | | |
| 75 Gyration | 7.20% | 2.401 |
| 65 Gyration | 7.70% | 2.383 |
| 50 Gyration | 8.30% | 2.370 |

4.3 Rutting Performance

The average rut resistance performance results using the Asphalt Pavement Analyzer for the Rugby, Eddy, Fargo, and Grand Forks project mixes are shown in Tables 25, 26, 27, and 28. Figure 36 displays a summary of the rut results of all the projects. The dashed line in Figure 36 indicates the rutting failure criterion of 7 mm for low level pavements. Rut failure occurs when rut values exceed the 7, 8, or 9-mm thresholds for low, medium, and high-level pavements, respectively.

Table 25. Rut Resistance Performance Summary for the Rugby Mix

| | AC Binder | Average (mm) | SD (mm) | COV (%) |
|-------------|-----------|--------------|---------|---------|
| 75 Gyration | 58H-28 | 2.58 | 0.37 | 14.5% |
| 65 Gyration | 58H-28 | 3.45 | 0.42 | 12.0% |
| 55 Gyration | 58H-28 | 3.82 | 1.15 | 30.1% |

Table 26. Rut Resistance Performance Summary for the Eddy Mix

| | AC Binder | Average (mm) | SD (mm) | COV (%) |
|-------------|-----------|--------------|---------|---------|
| 75 Gyration | 58H-34 | 3.05 | 0.30 | 9.7% |
| 65 Gyration | 58H-34 | 3.91 | 0.96 | 15.5% |
| 55 Gyration | 58H-34 | 4.67 | 0.25 | 5.3% |

Table 27. Rut Resistance Performance Summary for the Fargo Mix

| | AC Binder | Average (mm) | SD (mm) | COV (%) |
|-------------|-----------|--------------|---------|---------|
| 75 Gyration | 58S-28 | 4.20 | 1.17 | 27.9% |
| 65 Gyration | 58S-28 | 5.72 | 0.66 | 11.5% |
| 50 Gyration | 58S-28 | 6.60 | 0.78 | 11.8% |

Table 28. Rut Resistance Performance Summary for the GF Mix

| | AC Binder | Average (mm) | SD (mm) | COV (%) |
|-------------|-----------|--------------|---------|---------|
| 75 Gyration | 58S-28 | 4.33 | 1.40 | 32.3% |
| 65 Gyration | 58S-28 | 4.47 | 0.43 | 9.6% |
| 50 Gyration | 58S-28 | 7.03 | 0.63 | 8.9% |

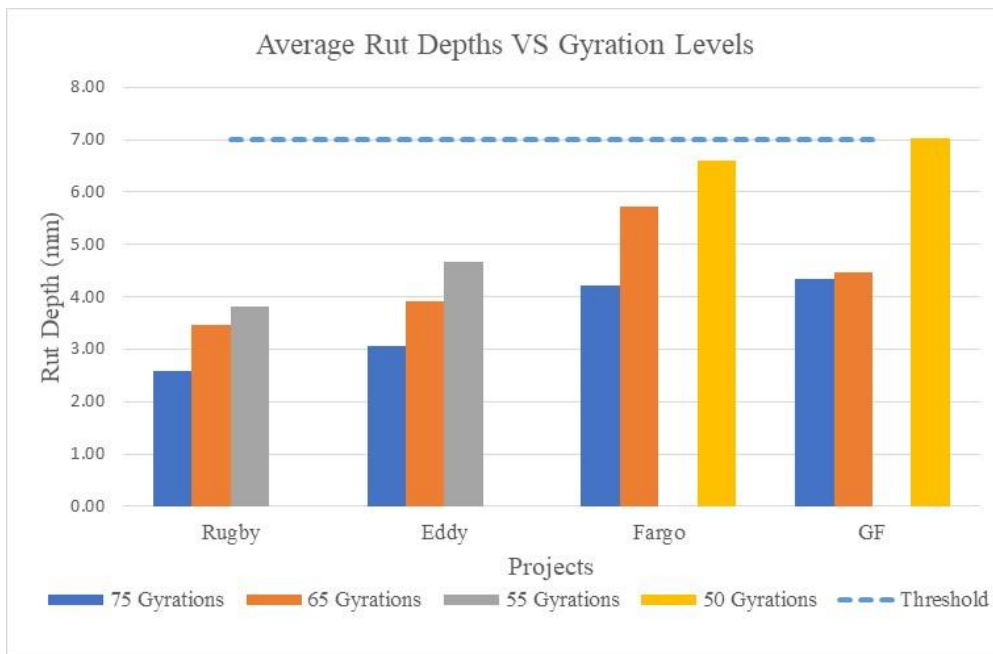


Figure 36. Average Rut Resistance Performance Summary

Observing the rut test results, one can see that for each project, rut values increase by decreasing the number of gyrations. The rate of increase of rut depth with decrease in number of gyrations from 75 to 65 was little over 30% for all the project mixes except for Grand Forks mix (3%). Decrease of gyrations from 75 to 55 or 50 gyrations resulted in rut increase of little over 50%. Rut values increase due to decrease in number of gyrations were higher in the Fargo and Grand Forks mixes compared to the Rugby and Eddy mixes, where Rugby and Eddy mixes had higher FAA values (45) compared to Fargo and Grand Forks project mixes with FAA values of 43 and 40, respectively. Also, Rugby and Eddy mixes had higher polymer content than the Fargo and Grand Forks project mixes. Rugby and Eddy mixes had average rut depth values much less than the 7 mm rut threshold criterion for all gyration levels. Rut depths for the 50-gyration level for Fargo and Grand Forks were about 7 mm and less than the 8- and 9-mm thresholds. This means that even though lowering the gyration level decreased rut resistance, it stayed at acceptable levels.

4.4 Low Temperature Cracking Performance

Fracture energy in the range of 350 – 400 J/m² is considered borderline, and permissible on less critical pavements (Newcomb, 2018). The average results of low temperature tests (DCT) for the Rugby, Eddy, Fargo, and GF project mixes are shown in Tables 29, 30, 31, and 32.

Table 29. Low Temperature Performance DCT Test Summary Results - Rugby

| | AC Binder | Average (J/m ²) | SD (J/m ²) | COV (%) |
|-------------|-----------|-----------------------------|------------------------|---------|
| 75 Gyration | 58H-28 | 561.50 | 15.29 | 2.7% |
| 65 Gyration | 58H-28 | 621.75 | 102.98 | 16.6% |
| 55 Gyration | 58H-28 | 587.00 | 24.14 | 4.1% |

Table 30. Low Temperature Performance DCT Test Summary Results - Eddy

| | AC Binder | Average (J/m ²) | SD (J/m ²) | COV (%) |
|-------------|-----------|-----------------------------|------------------------|---------|
| 75 Gyration | 58H-34 | 445.25 | 32.57 | 7.3% |
| 65 Gyration | 58H-34 | 494.00 | 48.33 | 9.8% |
| 55 Gyration | 58H-34 | 498.75 | 45.57 | 9.1% |

Table 31. Low Temperature Performance DCT Test Summary Results - Fargo

| | AC Binder | Average (J/m ²) | SD (J/m ²) | COV (%) |
|-------------|-----------|-----------------------------|------------------------|---------|
| 75 Gyration | 58S-28 | 593.25 | 105.05 | 17.7% |
| 65 Gyration | 58S-28 | 393.25 | 105.07 | 26.7% |
| 50 Gyration | 58S-28 | 627.50 | 83.82 | 13.4% |

Table 32. Low Temperature Performance DCT Test Summary Results - GF

| | AC Binder | Average (J/m ²) | SD (J/m ²) | COV (%) |
|-------------|-----------|-----------------------------|------------------------|---------|
| 75 Gyration | 58S-28 | 503.00 | 45.37 | 9.0% |
| 65 Gyration | 58S-28 | 415.67 | 58.03 | 15.0% |
| 50 Gyration | 58S-28 | 1296.00 | 704.30 | 65.8% |

The observed low temperature cracking results indicate that the Rugby and Eddy mixes satisfied the minimum fracture energy of 400 J/m² for all gyration levels. For the Fargo mix, all samples passed except for two 65 gyrations samples pulling the average energy for 65 gyrations marginally below 400 J/m². For the Grand Forks mix, all samples passed except for one 65 gyrations sample and one 50 gyrations sample. Since the other three 65 gyrations samples were clustered above the 400 J/m² mark and the failed sample is very low (301 J/m²), it can be considered an outlier, thus ignored. For the 50 gyrations samples, one sample came below the 400 J/m² mark while the other three samples were much higher, thus the fourth sample will be ignored.

The highest average fracture energy is 1296 J/m² for the Grand Forks 50 gyrations mix with asphalt binder of 58S-28 and 8.3% binder content. For Rugby and Eddy mixes, fracture energy increased for 65 gyrations but for 55 gyrations, fracture energy slightly decreased for Rugby and slightly increased for Eddy compared to the energy of 65 gyrations but both remained higher than the energy of the 75 gyrations. On the other hand, for Fargo and Grand Forks mixes, the average energies for 65 gyrations decreased compared to 75 gyrations, but significantly increased for 50 gyrations.

Since fracture energy is the main indicator for resistance to low temperature cracking, the 55 and 50 gyration levels with higher energy results indicate better performance for all the mixes. Average energies for all the mixes were comparable except for the Grand Forks mix at 50 gyrations and 8.3% binder content, therefore, it is difficult to make judgment on mix performance based on binder grade. Figure 37 summarizes the low temperature cracking performance results and Figure 38 displays the before and after DCT testing of a sample. The dashed line in Figure 37 indicates minimum fracture energy value (400 J/m²) to pass a sample.

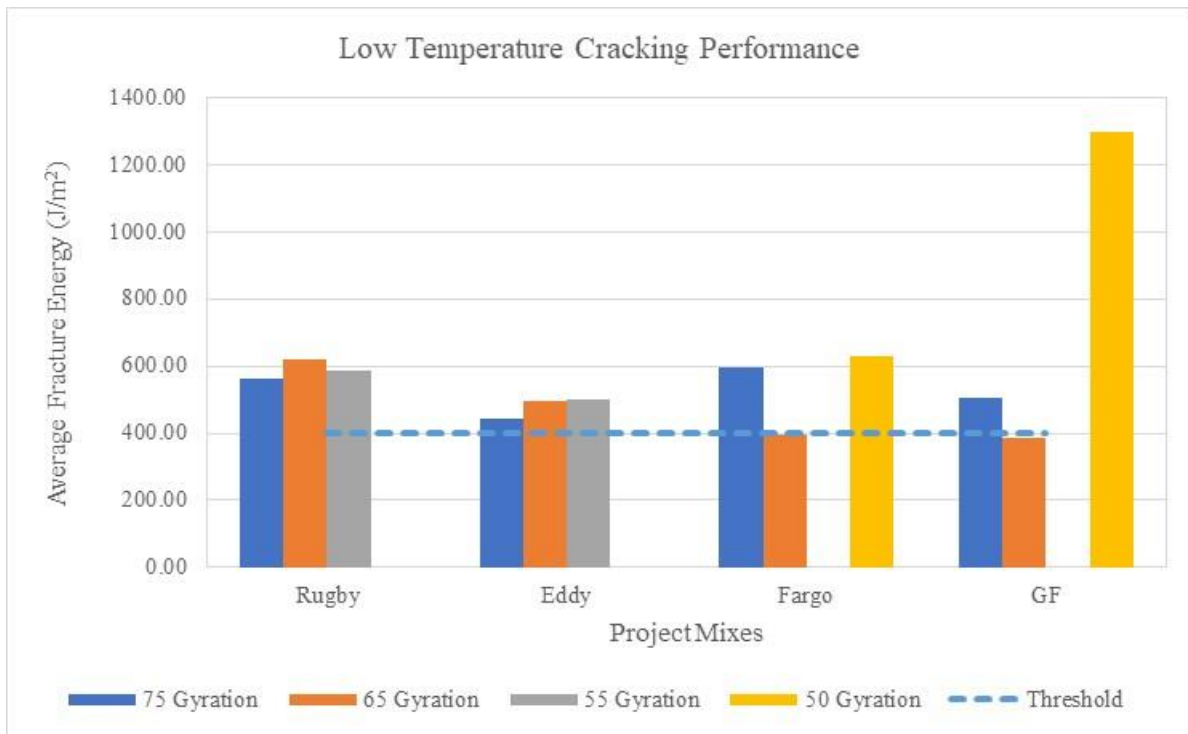


Figure 37. Overall Low Temperature Cracking Performance Results



Figure 38. Typical Before and After DCT Test Samples

4.5 Fatigue Cracking Performance

Tables 33 through 36 display summaries of average fracture energies and flexibility indices for the four mixes (Rugby, Eddy, Fargo, and Grand Forks). Figures 39 and 40 show the average fatigue cracking and FI performances, respectively. The dashed line in Figure 40 indicates the minimum FI value to be accepted.

Table 33. Fatigue Cracking and FI Performance Summary - Rugby

| | AC Binder | Average Fracture Energy (J/m ²) | FI |
|-------------|-----------|---|-------|
| 75 Gyration | 58H-28 | 2917.23 | 15.87 |
| 65 Gyration | 58H-28 | 2678.09 | 12.49 |
| 55 Gyration | 58H-28 | 2920.91 | 19.05 |

Table 34. Fatigue Cracking and FI Performance Summary - Eddy

| | AC Binder | Average Fracture Energy (J/m ²) | FI |
|-------------|-----------|---|-------|
| 75 Gyration | 58H-34 | 1773.02 | 14.24 |
| 65 Gyration | 58H-34 | 2017.32 | 19.37 |
| 55 Gyration | 58H-34 | 1947.14 | 16.28 |

Table 35. Fatigue Cracking and FI Performance Summary - Fargo

| | AC Binder | Average Fracture Energy (J/m ²) | FI |
|-------------|-----------|---|-------|
| 75 Gyration | 58S-28 | 1766.00 | 7.05 |
| 65 Gyration | 58S-28 | 2165.25 | 15.46 |
| 50 Gyration | 58S-28 | 2189.50 | 13.81 |

Table 36. Fatigue Cracking and FI Performance Summary - GF

| | AC Binder | Average Fracture Energy (J/m ²) | FI |
|-------------|-----------|---|-------|
| 75 Gyration | 58S-28 | 1889.25 | 8.72 |
| 65 Gyration | 58S-28 | 2111.75 | 15.21 |
| 50 Gyration | 58S-28 | 2449.50 | 24.38 |

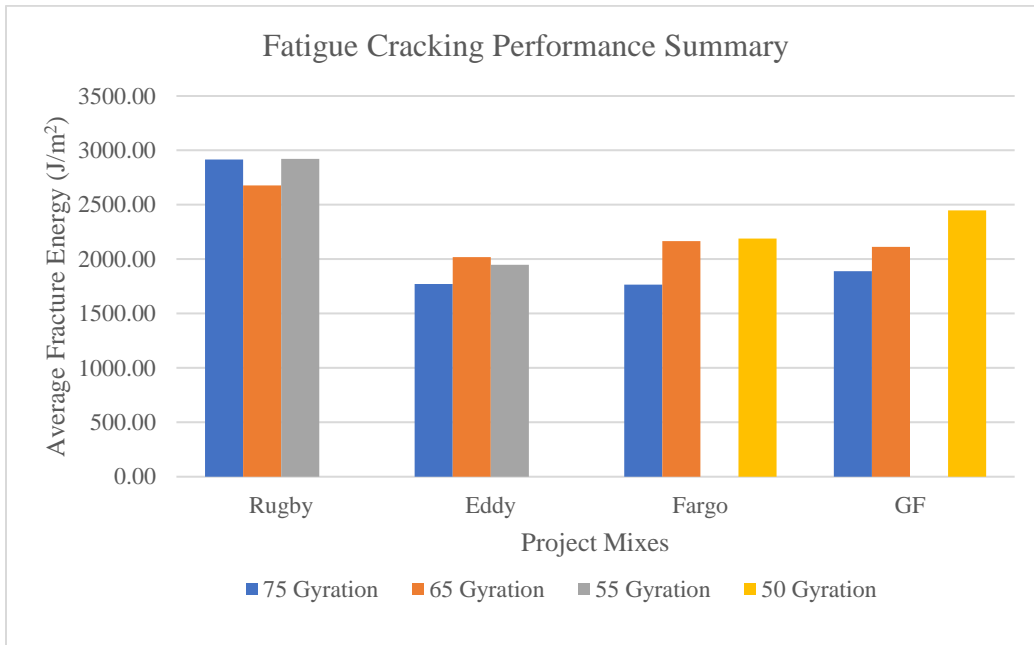


Figure 39. Fatigue Cracking Performance Summary

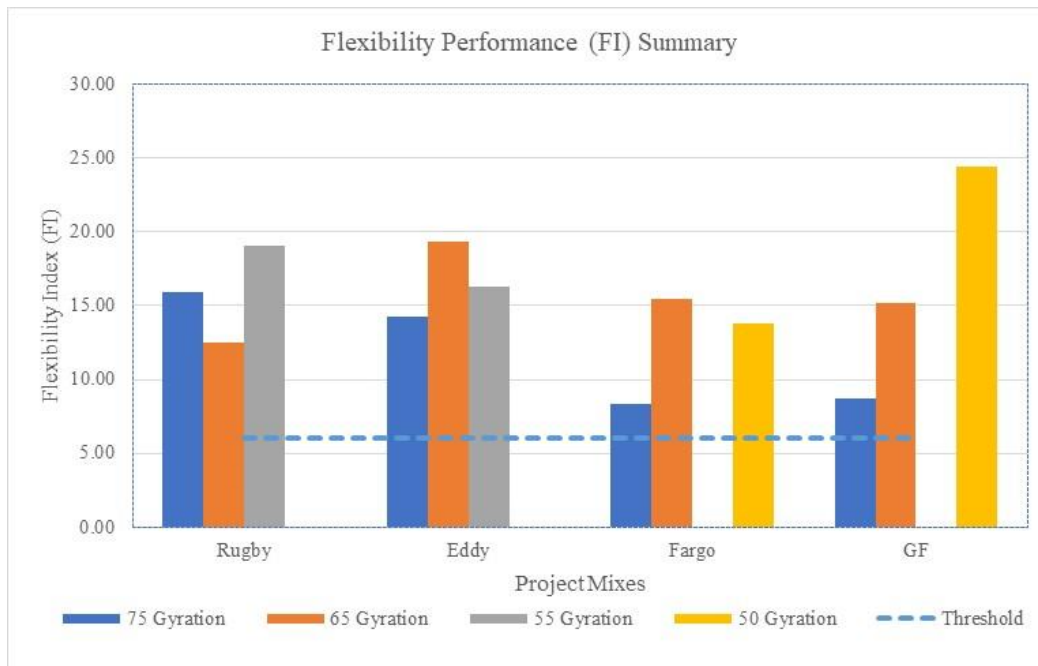


Figure 40. Flexibility Index (FI) Performance Summary

Looking at the IFIT results of fracture energy and Flexibility Indices of the SCB test, one can see a general trend of an increase in fracture energy and FI values with decrease in gyration levels (i.e. increase in binder content). For Rugby, fracture energy and FI values dip for the 65 gyrations then increase again for the 55 gyrations. On the other hand, fracture energy and FI spike for the 65 gyrations in Eddy project then slightly ease out for the 55 gyrations. Fracture energy values of the Rugby mix for all gyration levels were higher than fracture energy values for the remaining mixes. Since the FAA values and gradations of Rugby and Eddy mixes were in close proximity, the only major difference between Rugby and Eddy mixes was the binder grade. The Grand Forks mix at 50 gyrations, where binder content is highest (8.3%), produced the largest FI value for all the mixes. Figure 41 shows the typical sample specimen after SCB test is performed.



Figure 41. Typical Sample After SCB Test

4.6 Statistical Analysis

The statistical Analysis of Variance (ANOVA) was performed on the APA rut resistance results, the low temperature cracking (DCT fracture energy) results, and the fatigue cracking (SCB Flexibility Index) results. The results were grouped in three subgroups: high gyration level (75 gyrations), Medium gyration level (65 gyrations), and low gyration level (either 55 or 50 gyrations). The null hypothesis is given as, H_0 : the means of the results are equal. On the other hand, the alternate hypothesis, H_1 : the means of the results are not equal. Rejection of the null hypothesis indicates that the results are significantly different and can be compared.

The ANOVA single factor statistical analysis of the APA rutting results is presented in Table 37. Observation of the statistical results indicates that the P-value is less than the significance value ($P = 0.00022 < 0.05$); therefore, the null hypothesis is rejected. This means that the results within each gyration level and across the three-gyration levels are significantly different and can be compared.

Table 37. Single Factor ANOVA Analysis on the APA Rutting Results

| SUMMARY | | | | | | |
|----------------------------|--------------|------------|----------------|-----------------|----------------|---------------|
| <i>Groups</i> | <i>Count</i> | <i>Sum</i> | <i>Average</i> | <i>Variance</i> | | |
| High Gyr. Level | 16 | 56.674 | 3.54212 | 1.30208 | | |
| Med. Gyr. Level | 16 | 70.1993 | 4.38746 | 1.00404 | | |
| Low Gyr. Level | 16 | 88.4471 | 5.52794 | 2.35612 | | |
| ANOVA | | | | | | |
| <i>Source of Variation</i> | <i>SS</i> | <i>df</i> | <i>MS</i> | <i>F</i> | <i>P-value</i> | <i>F crit</i> |
| Between Groups | 31.7801 | 2 | 15.8901 | 10.2247 | 0.00022 | 3.20432 |
| Within Groups | 69.9335 | 45 | 1.55408 | | | |
| Total | 101.714 | 47 | | | | |

The ANOVA single factor statistical analysis of the DCT fracture energy results is presented in Table 38. Observation of the statistical results indicates that the P-value is less than the significance value ($P = 0.02978 < 0.05$); therefore, the null hypothesis is rejected. This means that the results within each gyration level and across the three-gyration levels are significantly different and can be compared.

Table 38. Single Factor ANOVA Analysis on the DCT Fracture Energy Results

| SUMMARY | | | | | | |
|----------------------------|--------------|------------|----------------|-----------------|----------------|---------------|
| <i>Groups</i> | <i>Count</i> | <i>Sum</i> | <i>Average</i> | <i>Variance</i> | | |
| High Gyr. Level | 16 | 8412 | 525.75 | 6299.67 | | |
| Med. Gyr. Level | 16 | 8095 | 505.9375 | 21435 | | |
| Low Gyr. Level | 16 | 11486 | 717.875 | 145225 | | |
| ANOVA | | | | | | |
| <i>Source of Variation</i> | <i>SS</i> | <i>df</i> | <i>MS</i> | <i>F</i> | <i>P-value</i> | <i>F crit</i> |
| Between Groups | 438517.63 | 2 | 219258.8 | 3.80307 | 0.02978 | 3.20432 |
| Within Groups | 2594391.7 | 45 | 57653.15 | | | |
| Total | 3032909.3 | 47 | | | | |

The ANOVA single factor statistical analysis of the SCB Flexibility Index (FI) results is presented in Table 39. Observation of the statistical results indicates that the P-value is less than the significance value ($P = 0.00311 < 0.05$); therefore, the null hypothesis is rejected. This means that the results within each gyration level and across the three-gyration levels are significantly different and can be compared.

Table 39. Single Factor ANOVA Analysis on the SCB FI Results

SUMMARY

| <i>Groups</i> | <i>Count</i> | <i>Sum</i> | <i>Average</i> | <i>Variance</i> |
|-----------------|--------------|------------|----------------|-----------------|
| High Gyr. Level | 16 | 183.53 | 11.4706 | 20.0871 |
| Med. Gyr. Level | 16 | 250.13 | 15.6331 | 34.3144 |
| Low Gyr. Level | 16 | 309.86 | 19.3663 | 59.3848 |

ANOVA

| <i>Source of Variation</i> | <i>SS</i> | <i>df</i> | <i>MS</i> | <i>F</i> | <i>P-value</i> | <i>F crit</i> |
|----------------------------|-----------|-----------|-----------|----------|----------------|---------------|
| Between Groups | 499.219 | 2 | 249.609 | 6.581 | 0.00311 | 3.20432 |
| Within Groups | 1706.79 | 45 | 37.9288 | | | |
| Total | 2206.01 | 47 | | | | |

5. CONCLUSIONS AND RECOMMENDATIONS

Since all the results were statistically significant as shown by the single factor ANOVA statistical analysis, comparison and interpretation of the results for each test would be done with a high level of confidence. As expected, rut result values generally increased with decreased number of gyrations across all mixes. This indicates that the increase in binder content due to the increase of air voids as a result of lower compactive effort consistently resulted in relatively lower rut resistance mixes. The average rut values for Fargo and Grand Forks mixes were higher than the average rut values of Rugby and Eddy projects by 50% due to lower FAA and polymer content. Even-though all rut values were practically below the 7 mm threshold for all the mixes, Rugby and Eddy rut values were much smaller than the rut values of Fargo and Grand Forks mix results. This means that even though lowering the gyration level to accommodate durability has marginally increased rut values, the rut resistance performance stayed at acceptable levels. This compromise would be acceptable if the mixes with lower gyration levels result in improved durability, low temperature cracking, and fatigue cracking performances.

It has been established that the higher the fracture energy the better low temperature cracking performance. And since the fracture energies for 55 and/or 50 gyration levels were higher than those for 75 and 65 gyrations levels, one could conclude that resistance to low temperature cracking continued to improve with lower gyration levels for all the mixes indicating better performance.

For assessing fatigue cracking performance, Flexibility Index values were used for the evaluation. Previous research recommended minimum FI values of 6, 5, and 4 for fatigue cracking resistant mixes used on high, medium, and low-level corridor pavement mixes, respectively. In this project, Rugby and Eddy mixes represented high level mixes (FAA = 45), Grand Forks mix represented a medium level mix (FAA = 43), and the Fargo mix represented a low-level mix (FAA = 40). For this study, FI values ranged from 8.3 to 24.4 indicating that all mixes pass the FI threshold criteria for all pavement mix levels. For Eddy and Fargo projects, FI values peaked at the 65 gyrations level while for Rugby and Grand Forks project mixes, FI values peaked at the 55 and 50 gyration levels, respectively. As expected, when gyration levels were lowered, fatigue resistance improved due to improved flexibility (durability) of the mixes.

Overall, low temperature cracking and fatigue cracking resistance performances were better at 65 and 55 or 50 gyrations throughout the mixes. At the same time, even-though rut resistance performances decreased for the 65 and 55 or 50 gyration levels, rut resistances were still considered an acceptable compromise.

In developing balanced mix design gyrations, the following logic has been followed. Since rut resistance performance remained acceptable throughout the gyration levels, it became a non-factor in the evaluation. Therefore, the evaluation will be based on low temperature cracking and fatigue cracking resistance performances.

For convenience, Table 40 shows rutting, low temperature cracking, and fatigue cracking performance results for all the mixes and gyration levels. For the Rugby mix, the fracture energy for the 65 gyrations and 55 gyrations increased by 11% and 5%, respectively, compared to the 75 gyration's fracture energy. For fatigue cracking evaluation, the FI value decreased by 21% for the 65 gyrations and increased by 20% for the 55 gyrations. Since fracture energy peaked at 65 gyrations and the FI value at 55 gyrations is well above 6, the recommended design gyration for the Rugby mix is 65 gyrations.

Table 40. Rutting, LTC, and FC Performance for all Mixes and Gyration Levels

| Project & Gyration Level | Binder Grade | FAA | Rutting (mm) | Low Temp. Cracking Fracture Energy (J/m ²) | Fatigue Cracking (FI Index) |
|--------------------------|--------------|-----|--------------|--|-----------------------------|
| Rugby-75 | 58H-28 | 45 | 2.58 | 561.50 | 15.87 |
| Rugby-65 | | | 3.45 | 621.75 | 12.49 |
| Rugby-55 | | | 3.82 | 587.00 | 19.05 |
| Eddy-75 | 58H-34 | 45 | 3.05 | 445.25 | 14.24 |
| Eddy-65 | | | 3.91 | 494.00 | 19.37 |
| Eddy-55 | | | 4.67 | 498.75 | 16.28 |
| Grand Forks-75 | 58S-28 | 43 | 4.33 | 503.00 | 08.72 |
| Grand Forks-65 | | | 4.47 | 415.67 | 15.21 |
| Grand Forks-50 | | | 7.03 | 1296.00 | 24.38 |
| Fargo-75 | 58S-28 | 40 | 4.20 | 593.25 | 07.05 |
| Fargo-65 | | | 5.72 | 393.25 | 15.46 |
| Fargo-50 | | | 6.60 | 627.50 | 13.81 |

For the Eddy mix, the low temperature cracking resistance increased by 11% at 65 gyrations and by 12% at 55 gyrations compared to 75 gyrations. For fatigue cracking resistance performance, FI values increased by 36% and 14% for 65 and 55 gyration levels, respectively. But since low temperature resistance performance for the 65 and 55 gyrations were almost similar and the FI value for the 65 gyrations was higher than the 55-gyration level, the 65-gyration design is recommended for the Eddy mix.

For the Fargo mix, the low temperature cracking resistance is decreased by 34% at 65 gyrations and increased by 6% at 50 gyrations compared to 75 gyrations. For fatigue cracking resistance performance, FI values are increased by 119% and 96% for 65 and 50 gyration levels, respectively. Based on the two metrics, the 50-gyration design will be chosen for the Fargo mix.

For the Grand Forks mix, the fatigue cracking resistance is decreased 17% at 65 gyrations and increased by 158% at 50 gyrations compared to 75 gyrations. For fatigue cracking resistance performance, FI values are increased by 74% and 180% for 65 and 50 gyration levels, respectively. Based on the two metrics, the 50-gyration design will be chosen for the Grand Forks mix as a balanced mix design.

Therefore, the recommended N_{design} for the Rugby and Eddy mixes (high end pavements) is 65 gyrations while for Fargo and Grand Forks mixes (intermediate and low-end pavements), the recommended number of gyrations is 50.

6. REFERENCES

- Aguilar-Moya, J. P., Prozzi, J. A., & Tahmoressi, M. (2001). Optimum Number of Superpave Gyration Based on Project Requirements. *SAGE Journals*, 84-92.
- Al-Qadi, I., Ozer, H., Lambros, J., El Khatib, A., Singhvi, P., Khan, T., Doll, B. (2015). Testing Protocols to Ensure Performance of High Asphalt Binder Replacement Mixes using RAP and RAS. Urbana, IL: Illinois Center for Transportation.
- Aschenbrenner, T. (1995). Investigation of Low Temperature Cracking in Hot Mix Asphalt. Denver: Colorado Department of Transportation.
- Asphalt. (2013, January). Asphalt: The Magazine of the Asphalt Institute. Retrieved from Asphalt: <http://23.20.20.129/history-of-asphalt-mix-design-in-north-america-part-1/>
- Bradshaw, L. (2016, November 3). Sure-Seal Pavement Maintenance Inc. Retrieved from Transverse/ Thermal Cracking in Asphalt Pavement: Causes and Repair: <https://suresealpavement.com/blog/transversethermal-cracking-asphalt-pavement-causes-repair/>
- Coleri, E., Sreedhar, S., Haddadi, S., & Wruck, B. (2018). Adjusting Asphalt Mixes for Increased Durability and Implementation of a Performance Tester to Evaluate Fatigue Cracking of Asphalt. Corvallis: Oregon Department of Transportation.
- Cross, S., & Choho Lee, J. (2000). Evaluation of the Superpave Gyration Compactor for Low Volume Roads. Topeka, Kansas: Kansas University Center for Research, Inc.
- Diefenderfer, S., Bowers, B., & McGhee, K. (2018). Impact of Gyration Reduction and Design Specification Changes on Volumetric Properties of Virginia Dense-Graded Asphalt Mixtures. *Transportation Research Record*, 143-153.
- Gedafa, D., Berg, A., Karki, B., Saha, R., & Melaku, R. (2017). Cracking and Rutting Performance of Field and Laboratory HMA Mixes. *Airfield and Highway Pavements 2019: Testing and Characterization of Pavement Materials* (pp. 12-19). Philadelphia: American Society of Civil Engineers.
- Kandhal, P. S., & Mallick, R. B. (1999). Evaluation of Asphalt Pavement Analyzer for HMA Mix Design. Auburn: National Center for Asphalt Technology.
- Li, X., Marasteanu, M., & Turos, M. (2007). Study of Low Temperature Cracking in Asphalt Mixtures using Mechanical Testing and Acoustic Emission Methods. (pp. 427-453). *Asphalt Paving Technology: Association of Asphalt Paving Technologists - Proceedings of the Technical Sessions*.
- Li, X.-J., & Marasteanu, M. (2010). Using Semi Circular Bending Test to Evaluate Low Temperature Fracture Resistance for Asphalt Concrete. *Experimental Mechanics*, 867-876.
- Liley, C. (2018). *Rutting: Causes, Prevention, and Repairs*. Chicago: Illinois Asphalt Pavement Association.
- Marasteanu, M., Zofka, A., Turos, M., Li, X., Velasquez, R., Xue, L., Ojo, J. (2007). Investigation of Low Temperature Cracking in Asphalt Pavements: National Pooled Fund Study 776 . St. Paul: Minnesota Department of Transportation.
- Maupin, G., Transportation, V. D., & Council, V. T. (2003). Additional Asphalt to Increase the Durability of Virginia's Superpave Surface Mixes. Transportation Research Council. Minnesota Department of Transportation. (2014). MnDOT. Retrieved from Road Research : Low Temperature Cracking in Asphalt Pavements: http://www.dot.state.mn.us/mnroad/projects/Low_Temp_Cracking/

- Moghaddam, T., Karim, M., & Abdelaziz, M. (2011). A review on Fatigue and Rutting performance of asphalt mixes. *Scientific Research and Essays*, 670-682.
- Monismith, C., Finn, F., & Vallerger, B. (1989). *A Comprehensive Asphalt Concrete Mixture Design System*. ASTM International: Asphalt Concrete Mix Design: Development of More Rational Approaches.
- National Center for Asphalt Technology. (2017, January). Moving Towards Balanced Mix Design for Asphalt Mixtures. Retrieved from National Center for Asphalt Technology at Auburn University: <http://eng.auburn.edu/research/centers/ncat/newsroom/2017-spring/balanced-mix.html>
- NDDOT. (2020). *Standard Specifications for Road and Bridge Design*, North Dakota Department of Transportation, Bismarck, North Dakota.
- Nsengiyumva, G., Yong-Rak, K., & You, T. (2015). Development of Semicircular Bend (SCB) Test Method for Performance Testing of Nebraska Asphalt Mixtures. Nebraska: Nebraska Department of Roads.
- Ohio Asphalt. (2004, Summer). Ohio Asphalt. Retrieved from Flexiblepavement.org (2018 August 1): http://www.flexiblepavements.org/sites/www.flexiblepavements.org/files/ohio-asphalt-pdf/newsletter_37.pdf
- Pavement Interactive. (2009). Superpave Mix Design. Retrieved from Pavement Interactive: <https://www.pavementinteractive.org/reference-desk/design/mix-design/superpave-mix-design/>
- Prowell, B., & Brown, R. (2007). *Superpave Mix Design: Verifying Gyration Levels in the Ndesign Table*. Auburn, AL: National Cooperative Highway Research Program (NCHRP Report 573).
- Qarouach, S., Khosla, P., & Ayyala, D. (2015). *An Investigation of the Effect of Ndesign Values on Performance of Superpave Mixtures*. Raleigh: North Carolina State University.
- Roberts, F., Mohammad, L., & Wang, L. (2002). History of Hot Mix Asphalt Mixture Design in the United States. *Materials in Civil Engineering: American Society of Civil Engineers*, 279-293.
- Saha, G., & Biligiri, K. (2012). Fracture properties of asphalt mixtures using semi-circular bending test: A state-of-the-art review and future research. Elsevier: *Construction and Building Materials*, 103-112.
- Saha, R., Karki, B., Berg, A., Melaku, R., & Gedafa, D. (2017). Effect of RAP on Cracking and Rutting Resistance of HMA Mixes. *Airfield and Highway Pavements 2017* (pp. 86-94). American Society of Civil Engineers.
- Shelquist, R., O'Connor, E., & Jordison, D. (1981). *Transverse Cracking Study of Asphalt Pavement*. Ames: Highway Division: Iowa Department of Transportation.
- Skok, E., Johnson, E., & Amir, T. (2000). *Asphalt Pavement Analyzer (APA) Evaluation*. St. Paul: Minnesota Department of Transportation Office of Research Services.
- Suleiman, N. (2005). *Evaluation of North Dakota's Asphalt Cement Binder Properties and Performance in Locally Produced HMA Mixtures*. Grand Forks: University of North Dakota Department of Civil Engineering.
- Wagoner, M., Buttlar, W., & Paulino, G. (2005). Disk-shaped Compact Tension test for Asphalt Concrete Fracture. *Experimental Mechanics*, 270-277.
- Washington Asphalt Pavement Association. (2010). asphaltwa.com. Retrieved from Washington Asphalt Pavement Association: <http://www.asphaltwa.com/rutting/>

- West, R., Rodenzo, C., Leiva, F., & Yin, F. (2018). Development of a Framework for Balanced Mix Design. Auburn: National Cooperative Highway Research Program (NCHRP) Project NCRHP 20-07.
- Williams, C., Buss, A., Mercado, G., Lee, H., & Bozorgzad, A. (2016). Validation of Gyratory Mix Design in Iowa. Ames: Institute for Transportation: Iowa State University.
- Yeo, Y. (2018). Evaluating and Improving Asphalt Pavement in the City of Pittsburgh. Department of Civil and Environmental Engineering: Carnegie Mellon University.